Article

Analytical Study Regarding the Seismic Response of a Moment-Resisting (MR) Reinforced Concrete (RC) Frame System with Reduced Cross Sections of the RC Beams

Ion Sococol [1], Petru Mihai [2,*], Tudor-Cristian Petrescu [2], Florin Nedeff [3,*], Valentin Nedeff [4] and Maricel Agop [5,6]

[1] Faculty of Civil Engineering and Building Services, "Gheorghe Asachi" Technical University of Iasi, 43 Dimitrie Mangeron Boulevard, 700050 Iasi, Romania; ion.sococol@student.tuiasi.ro

[2] Department of Concrete, Materials, Technology and Management, Faculty of Civil Engineering and Building Services, "Gheorghe Asachi" Technical University of Iasi, 43 Dimitrie Mangeron Boulevard, 700050 Iasi, Romania; tudor.petrescu@tuiasi.ro

[3] Department of Environmental Engineering and Mechanical Engineering, Faculty of Engineering, "Vasile Alecsandri" University of Bacău, 600115 Bacau, Romania

[4] Department of Industrial Systems Engineering and Management, Faculty of Engineering, "Vasile Alecsandri" University of Bacău, 600115 Bacau, Romania; vnedeff@ub.ro

[5] Department of Physics, Faculty of Machine Manufacturing and Industrial Management, "Gheorghe Asachi" Technical University of Iași, 700050 Iasi, Romania; m.agop@yahoo.com

[6] Academy of Romanian Scientists, 050094 Bucharest, Romania

* Correspondence: petru.mihai@academic.tuiasi.ro (P.M.); florin_nedeff@yahoo.com (F.N.)

Abstract: In the last few decades, a series of earthquakes were recorded which pointed out several deficiencies regarding the ductile seismic response of MR RC frame structures. Thus, the research problem centres around the failure mechanisms registered by the structures, which differ from the general notions of seismic response commonly found in current design standards and norms regarding seismic actions. In these conditions, in the present paper—by using comparative methods—the analytical validation of the solution of plastic hinge concentration and seismic energy dissipation in the marginal beam areas is proposed. Therefore, the RC beam sections were reduced (weakened) in the marginal areas which exhibit a plastic deformation potential, as well as in the corner areas of concrete slabs with vertical rectangular holes. The significant outcomes of this research imply the partial "guiding" of plastic hinges in the zones adjacent to beam ends. Furthermore, a reduction of both the negative effects of horizontal rigidization of the beams and the cracking and plastic deformation effects of beam-column frame joints was observed. With these technical implications, a complex mechanism of plastic deformation of MR RC frame models is registered in which all lateral elements (including RC columns) participate in the dissipation of seismic energy, without the occurrence of the "weak storey" mechanism for any of the analytical RC frame models. Furthermore, it is possible to observe the partial formation of the global plastic mechanism "Strong Columns—Weak Beams" (SCWB) for some of the structural models. Finally, the analytically studied innovative element regarding the improvement of the seismic response of pure MR RC frame structures is successfully validated.

Keywords: RC frame system; push-over analysis; reduced cross section; vertical holes; plastic hinges

1. Introduction

The Moment-Resisting (MR) Reinforced Concrete (RC) frame structures designed according to the ductile concept represent a class of lateral systems exhibiting a complex seismic response to severe dynamic loads.

The general mechanisms of structural deformation imply plastic deformations in the marginal beam areas (considered as main dissipative elements) and in the inferior areas for ground storey columns (see Figure 1b). There also exists the possibility of plastic hinges

occurrence in superior end areas for columns situated at the top storey. It is also possible for the plastic hinges to appear at both columns' ends for intermediate storeys, as long as the storey itself fulfils the stability conditions [1–3]. In these types of structures, the columns are considered non-dissipative lateral elements with local, minor (insignificant) plastic deformations. The same specifications are attributed both to beam-column frame joints and to RC slabs. In these conditions, the beam-column frame nodes form a common body with RC columns and the RC slab ensures the transfer of storey inertial forces through the beams and towards the vertical structural elements [1–9].

This capacity design concept, commonly used for current seismic design norms for pure MR RC frame structures [1,2], leads to the development of the global seismic response mechanism known as "Strong Columns—Weak Beams" (SCWB) [3–7].

Thus, in the following chapters, conceptual aspects that highlight the non-correspondence between the seismic response of pure MR RC frame systems and the elements specified in current seismic design norms for studies with several implications are discussed as follows:

1. Theoretical and analytical ones;
2. Experimental ones;
3. Real ones for RC frame structures which collapsed as a result of in situ severe seismic loading.
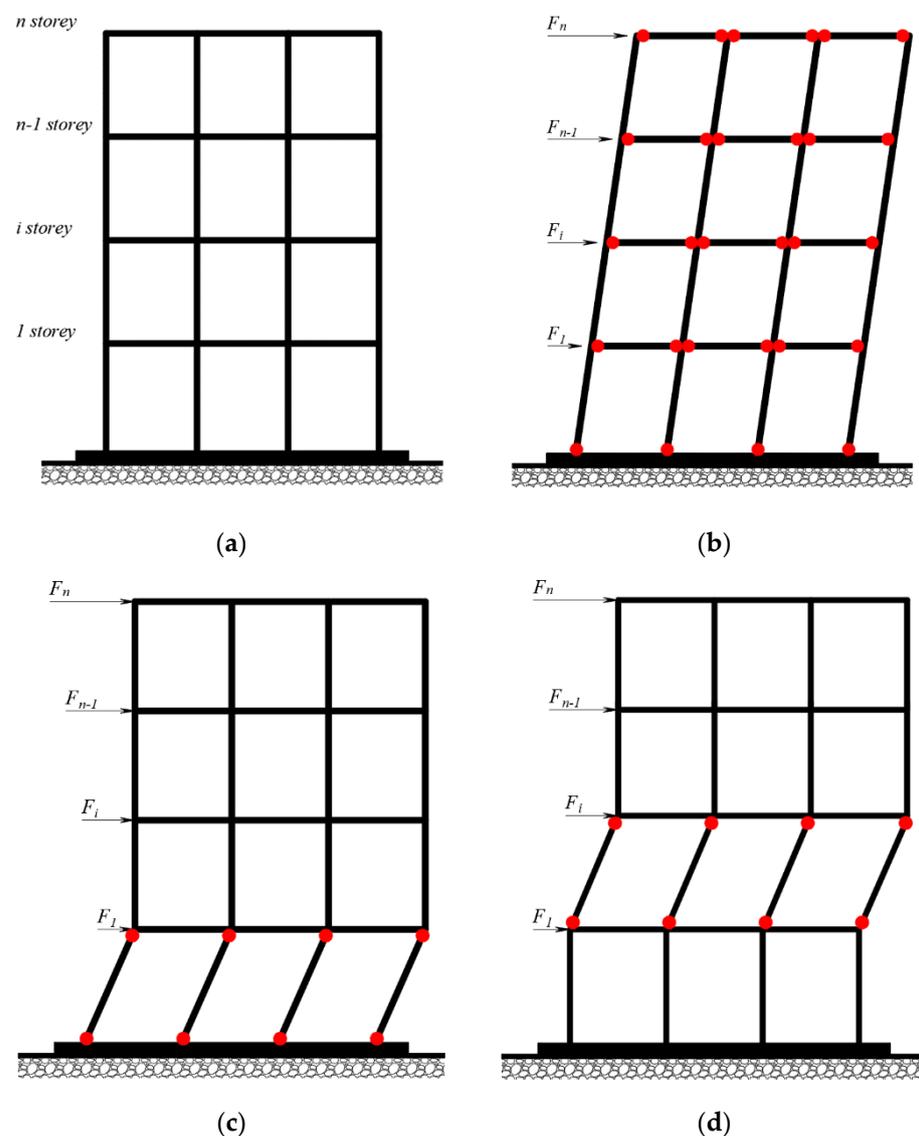

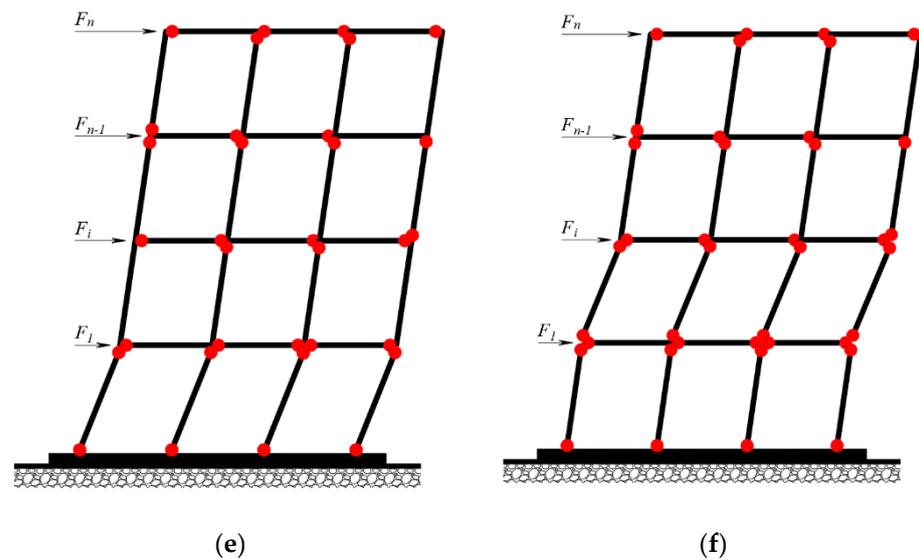(a)   (b)

(c)   (d)

Figure 1. *Cont.*

(**e**)　　　　　　　　　　　　　　　　　　　(**f**)

Figure 1. (**a**) Structural representation of the pure seismic resistant RC frame system, without lateral loading; (**b**) "The idealized global seismic response of the pure Moment Resisting (MR) Reinforced Concrete (RC) frame structure specified in current seismic design standards and structural engineering literature" (**S**trong **C**olumns—**W**eak **B**eams (SCWB) ductile mechanism) [1,2]; Fragile failure mechanism: (**c**) weak ground floor; (**d**) weak storey, registered both in analytical and experimental studies as well as in real RC frame structures, which underwent severe seismic actions; (**e**,**f**) Hybrid failure mechanisms (having, as an effect, the formation/development of plastic hinges at beam and column ends), registered both in analytical and experimental studies as well as in real RC frame structures, which underwent severe seismic actions.

As such, the objective of the current study is to underline, through available literature sources [8,9], the incapacity of the current MR RC frame systems—designed according to the ductile concept—to dissipate the seismic energy in accordance with the current seismic norms and to analytically validate a novel solution of plastic hinge concentration and seismic energy dissipation in the marginal beam areas.

2. Methodology

The research methodology pertaining to the current research paper implies four distinct stages:

I.　The establishment of the seismic response of MR RC frame systems through analytical and theoretical studies;

II.　The establishment of the seismic response of MR RC frame systems through the real, recorded seismic response of in situ structures subjected to severe earthquake actions;

III.　The obtainment of relevant conclusions and their overlap with the specifications of the current seismic design norms [1,2];

IV.　The proposal of solutions for improving the seismic response of existing and future MR RC frame systems by means of reducing the section of the beams in marginal areas.

The obtained results were studied by employing the comparative method.

3. Seismic Response of the MR RC Frame Structures through Theoretical and Analytical Implications

Within a complex (research) analytical study, carried out by Sococol et al. [10–15] and performed with ATENA 3D computer software [16], the seismic response for a series of MR RC frame models, reduced at a scale of 1:2 according to similitude criteria (rules), was studied [17–19]. Within this study, the longitudinal reinforcement percentages of the beams and columns, the reinforcement percentages of the slabs, the transversal beam and slab sections, the concrete strength classes, etc., were all varied. However, the inter-axis

dimensions and the height regime of the openings, for all types of structural models, were preserved.

As such, several different local and global structural deformation mechanisms were observed (see Figure 1c–f), with a different plasticisation mechanism presented in current seismic design norms [1,2] for seismically resistant RC frame structures.

Thus, for all RC frame models, plastic deformations were registered in end (marginal) zones of the columns, with intense concrete cracking and early reinforcement "yielding" (in tensioned areas) [10]. Consequently, the columns are presented as dissipative lateral elements which can lead to the occurrence of the unwanted "weak storey" mechanism (see Figure 1c–f).

The RC beams form a common rigid block with the slab and beam-column joints, "beams-slab-frame nodes", which influences the direction and occurrence of plastic hinges in marginal zones of the columns, in the area immediately adjacent to beam-column frame nodes. Additionally, the cracking process of the slab was observed. This process "decides" the marginal deformation length of the concrete beam [10–13,15]. Moreover, the RC slab controls the plastic rotation mode of the beams as well as the concentration of main tensions and specific deformations in concrete and reinforcement bars [10].

In these circumstances, the beams are presented as lateral dissipative elements but not as main seismic energy dissipative elements. Consequently, no (global) ductile mechanism "Strong Columns—Weak Beams" (SCWB), characteristic of pure seismic resistant RC frame structures, was registered (observed) [10–13,15] (Figure 2).

(a)

(b)

(c)

(d)

Figure 2. The effects of earthquakes in: (**a**) The Aegean Sea (2020), Izmir, Turkey (Reprinted from [20]); (**b**) Ecuador (2016) (Reprinted from [21]); (**c**) Ecuador (2016) (Reprinted from [22]); (**d**) Kobe (1995), Japan (Reprinted from [23]).

The RC beam-column joints did not have the performance specified in current seismic design norms, such as: nodes do not crack, their behaviour is in the linear elastic domain, they are a component part of the columns [1,2]. Rather, they crack intensively and become a "common body" with the beams and the RC slab [10–13,15].

Basically, for all the pure MR RC frame models on which non-linear static analysis (with ATENA 3D computer software, version 5.1.2.11514, Cervenka Consulting Ltd., Prague, Czech Republic [16]) was performed, a complex seismic energy dissipation mechanism was registered. This mechanism is formed through an active participation of all the lateral elements (beams, slabs, beam-column frame joints, columns) to the global seismic response. As such, reinforcement yielding and concrete cracking can be observed, together with concentration effects of the principal and tangential tensions and together with ultimate specific deformations of both concrete and reinforcement bars in the marginal areas of RC columns. The effects of these complex structural deformation processes lead to the occurrence of "weak storey" mechanisms.

Other non-linear static and dynamic studies [24–26] present the same local mechanisms of plastic hinge formation in marginal areas of the columns, which are:

- considering the rigid slab in the horizontal plane (for rigid-type floor) [27];
- not considering (using) the RC slab in extreme load conditions (having, as an effect, the fragile failure of the beams and the brittle failure of the columns) [28,29], etc.

Therefore, in most analytical and experimental studies, as well as in situations where real earthquakes occurred (see Figure 2 and collapsed RC frame structures for Wenchuan earthquake and Chi-chi earthquake in the research study conducted by Hu et al. [30], etc.), the following aspects were observed, regarding the seismic response of RC frame structures:

- fragile failure mechanisms of the structural system, through active plasticisation of the RC columns from a certain storey, in their superior and inferior (marginal) areas (Figure 1c,d and Figure 2);
- hybrid failure mechanisms (which have, as a specificity, the random formation/ development of plastic hinges at beam and column ends), which can take a multitude of forms (ex.: Figure 1e,f and Figure 2).

Related to the analytical studies, in seismic design codes, several suggestions and conclusions regarding the capacity design concept of pure MR RC frame structures were observed:

Thus, in the FEMA P-2012 norm [28,31], "two important suggestions regarding **S**trong **C**olumns—**W**eak **B**eams (SCWB) seismic energy dissipation mechanism (Figure 1b) for pure **M**oment **R**esisting (MR) **R**einforced **C**oncrete (RC) frame systems are specified" [32]:

- there is a possibility that the RC beams have a superior bending stiffness compared to the RC columns [11];
- it is proposed to use a higher base shear force than the value resulting from the calculation [33], in order to minimise the consequences of design deficiencies [34].

These suggestions and conclusions found in FEMA P-2012 [31] were taken into account and were practically applied through the seismic design methodology of pure MR steel frame systems, in accordance with P100-1 Romanian seismic design norms [1].

Thus, the steel columns are computed with a different set of lateral seismic forces (generated from the load groupings stage) than the ones for the frame beams, this represents a theoretical solution for the reduction of seismic effects on these types of structures (MR steel frames and MR RC frame systems) [32].

A final aspect to consider regarding the non-ductile seismic response of pure MR RC frame systems is that these types of structures are retrofitted in Japan. Thus, a shift is made by "changing the structural system from RC frames to coupled RC walls" [35]. In effect, the existing columns are integrated into walls named "wing walls" [35].

4. Real Seismic Response of MR RC Frame Structures and Experimental Research

"The seismic activity from the last two decades" [36] proves, for a large number of situations, the incapacity of development for the ductile deformation mechanism (represented in Figure 1b) for MR RC frame structures.

When confronted with real earthquakes, the issues regarding the capacity design concept and the seismic response of these types of structures become more acute when faced with the fact that their in situ structural response remains the main objective source of data regarding the performance of their seismic design.

Thus, for MR RC frame structures, designed with current seismic regulation norms, fragile seismic energy dissipation mechanisms were recorded (see Figure 1c,d and Figure 2), which manifested through the brittle failure of columns at a certain storey (see Figure 2a,b,d) or through a combination of hybrid failure mechanisms (see Figure 1e,f and Figure 2c)—"weak storey".

In essence, "the seismic activity from the last two decades" [36] revealed the necessity for the re-evaluation of the capacity design concept for the aforementioned type of structural system.

In this context, by performing experimental studies on seismic platforms or in other technical conditions, checks of the failure mechanisms identified in MR RC frame structures were attempted to be performed.

These studies were made based on structural models scaled according to similitude criteria or based on Reinforced Concrete (RC) frame prototypes.

Thus, the main experimental study in this technical research branch is "Seismic platform testing of a P + 9E seismic resistant RC dual system (with mainly RC frames)—prototype in Japan" [37].

The purpose of this experimental study was twofold: from a theoretical perspective, the checking of the global seismic response specified in seismic design norms was performed; from a practical (real) perspective, the in situ study of the seismic response aspects was performed on real structures from the same category of structural systems (dual type with mainly RC frames).

The main conclusions regarding the seismic response of this reinforced concrete prototype are:

- Extreme cracking of the RC beam-column joint;
- Deformation of marginal areas of RC columns;
- Slab cracking in the areas of interaction with the RC walls;
- Structural deformation of the ground floor walls and in other areas along the height of the structure, etc.

In these circumstances, no global plastic hinge mechanism was registered on beam ends in the way that the idealised mode of structural deformation is presented in current seismic design norms (see Figure 1b) [1,2].

Other experimental studies performed by Wang et al. [38], Taheri et al. [39], Li et al. [40], Zembaty et al. [41], Kamath et al. [42], and Rizwan et al. [43] prove the same manner of concentration of the plastic deformations in the end zones of RC columns. The cracking mode, the confinement effect (concrete transversal reinforcement) and the local concrete deformation in the adjacent beam-column frame node are all highlighted.

In addition, the bending rigidisation effect of the RC beams, due to the presence of the concrete slab in its real form and with real geometrical dimensions, was observed in an experimental study carried out by Pohoryles et al. [44].

Three experimental studies carried out by Li et al. [45], Hou et al. [46], and Zhang et al. [47] on seismic platforms for RC frame structural models and for dual system models with mainly RC frames, reduced to scale according to similitude criteria, and noted the same effects regarding the incapacity of the plasticisation process of the beams in their marginal areas.

Important observations regarding the seismic behaviour of the beam-column frame node, which is a part of the MR RC frame system, were also made in the experimental studies of Liu et al. [48] and Hu et al. [30].

Thus, important cracks and degradations were observed in the beam-column frame node, which occurred under the incidence of the active concentration effects of the plastic deformations in marginal column areas and partially in the end areas of the RC beams.

5. Conclusions That Specify and Reinforce the Need for the Current Analytical Study

Analytical, experimental studies and the effects of earthquakes in the last two decades regarding the seismic response of MR RC frame structures demonstrate a fragile global mechanism of failure by brittle rupture of RC columns in marginal end areas. The RC columns are dissipative elements which crack intensively and do not perform in the linear elastic domain.

The RC beams form a common body with the slab and with the beam-column frame node, "lending" from the bending rigidity of the slab in the horizontal plane, thus rotating and cracking as long as the slab rotates. This leads to the formation of a common rigid block RC "beams-slab-frame nodes", which, during the seismic energy dissipation process, directs the formation of plastic hinges towards the marginal areas of the RC columns.

The RC beam-column frame nodes form a common body with the beams and the slab and intensely crack together with the end zones of the columns.

The "Strong Columns-Weak Beams" (SCWB) global ductile mechanism presented in the current seismic design norms for pure MR RC frame structures exposed to earthquake actions does not occur for the case of analytical and theoretical studies, nor for real-life structures undergoing moderate to severe earthquakes. As such, weak storey mechanisms are registered, with random deformation patterns.

6. Complex Static Non-Linear Analysis of the Representative Pure Moment Resisting (MR) Reinforced Concrete (RC) Frame Model

6.1. General Aspects

The results, conclusions and observations pertaining to analytical and experimental studies, as well as to the experience obtained following the study of the MR RC frame structures, thus pointed towards a non-satisfactory seismic response of such structures. Obviously, the necessity of finding practical solutions which can lead to the improvement of the "ductile seismic response" [49] for such structural systems was recognised.

Consequently, a series of numerical simulations using the computer program ATENA 3D [16,50], were performed, having as a representative analytical model the K_7 MR RC frame system (see Figure 3) (Table 1) [10,15]. Based on this structural system, the other analytical models were generated, which had as a necessary condition (and main purpose), the modification of the seismic behaviour characteristics of three reinforced concrete structural elements from the make-up of the structural system:

- Beams;
- Slabs;
- Columns.

In the present paper, the structural modifications pertaining to the RC beams are analysed and discussed.

Therefore, for the analytical MR RC frame models, the cross section of the beam was reduced through the vertical mechanical drilling process in the zones which have a plastic deformation potential. The obtained seismic response from these structures was overlapped by means of the comparative method, both with the seismic response of the representative K_7 MR RC frame model—which does not have any reduced beam cross section—as well as with the seismic response of the K_7_S_B_1 MR RC frame model—for which the cross sections of the beams and slabs were reduced through the vertical mechanical drilling process.
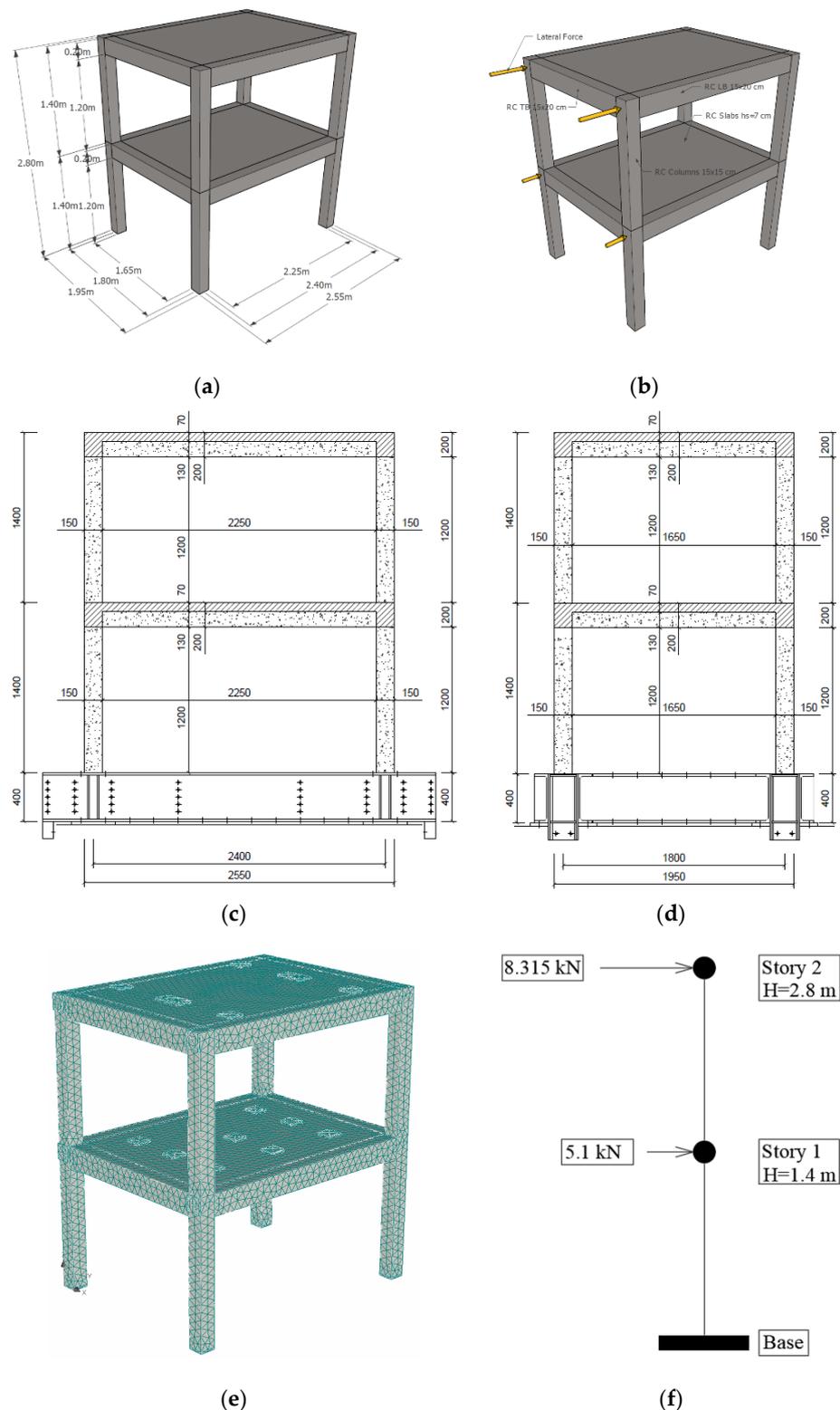
Figure 3. (**a**) Structure dimensions of the K_7 MR RC frame model; (**b**) Lateral loading consideration for pushover analysis of the K_7 MR RC frame system; (**c**,**d**) Representation of the longitudinal and transverse cross sections for K_7 MR RC frame system; (**e**) "Structural mesh discretization of the K_7 MR RC frame system" Reprinted from [13,15]; (**f**) Representation of the discrete system with lateral load consideration in the longitudinal direction for K_7 MR RC frame model. (Note: the way the lateral loads, the general geometric dimensions and the discretisation modes of the K_7 analytical model were considered is identical to the structural models specified in Table 1).

Table 1. Principal characteristic parameters considered in numerical analyses of the **M**oment **R**esisting (MR) **R**einforced **C**oncrete (RC) frame models.

NSC	CSC	LSRT	TSRT	LSR RC C [CS:15 × 15 cm]	LSR RC LB [CS:15 × 20 cm]	LSR RC TB [CS:15 × 20 cm]	TSR RC C	TSR RC LB and TB	R RC S [h_s = 7 cm]	GR
K_7	C20/25	Bst 500S	Bst 500M	4φ14	4φ8	4φ8	1φ4/1 CS	1φ4/1 CS	φ6	Figure 8(a2)
K_7_3_A	C20/25	Bst 500S	Bst 500M	4φ14	4φ8	4φ8	1φ4/1 CS	1φ4/1 CS	φ6	Figure 8(b2)
K_7_2_A	C20/25	Bst 500S	Bst 500M	4φ14	4φ8	4φ8	1φ4/1 CS	1φ4/1 CS	φ6	Figure 8(c2)
K_7_1_A	C20/25	Bst 500S	Bst 500M	4φ14	4φ8	4φ8	1φ4/1 CS	1φ4/1 CS	φ6	Figure 8(d2)
K_7_S_B_1	C20/25	Bst 500S	Bst 500M	4φ14	4φ8	4φ8	1φ4/1 CS	1φ4/1 CS	φ6	Figure 8(e2)

Note: NSC—**N**umerical **S**imulation **C**ode; CSC—**C**oncrete **S**trength **C**lass; LSRT—**L**ongitudinal **S**teel **R**einforcement **T**ype; TSRT—**T**ransverse **S**teel **R**einforcement **T**ype; LSR—**L**ongitudinal **S**teel **R**einforcement; RC—**R**einforced **C**oncrete; C—**C**olumns; CS—**C**ross **S**ection; LB—**L**ongitudinal **B**eams; TB—**T**ransverse **B**eams; TSR—**T**ransverse **S**teel **R**einforcement; R—**R**einforcement; S—**S**labs; h_s—slabs thickness; GR—**G**raphical **R**epresentation.

The MR RC frame models thus considered were laterally loaded with equivalent static forces (see Figure 3b,f), consequently allowing the obtainment of the "F-D" capacity curves together with the other types of curves. In addition, numerical values in a tabular form were obtained together with graphical representations of the deformation mode for each analytical RC frame model.

In essence, the present paper aims to validate the mechanical weakening (of resistance and lateral stiffness) method of dissipative structural elements—reinforced concrete beams—in the design stage, highlighting the emergence of the common rigid block "beams-slab-frame nodes" [51].

6.2. Input Data Consideration

The analytical MR RC frame models, reduced to a $\frac{1}{2}$ scale according to "similitude criteria" [17–19] from the present paper, were developed based on the K_7 representative structural system (see Figure 3a,c,d) and were laterally loaded with static forces at each storey level (Figure 3b,f). The numerical simulations for each structural model were made with the ATENA 3D computer program [16], having as input data the parameters specified in Tables 1 and 2. For reinforcement disposition, the representations in Figures 4–7 are to be consulted.
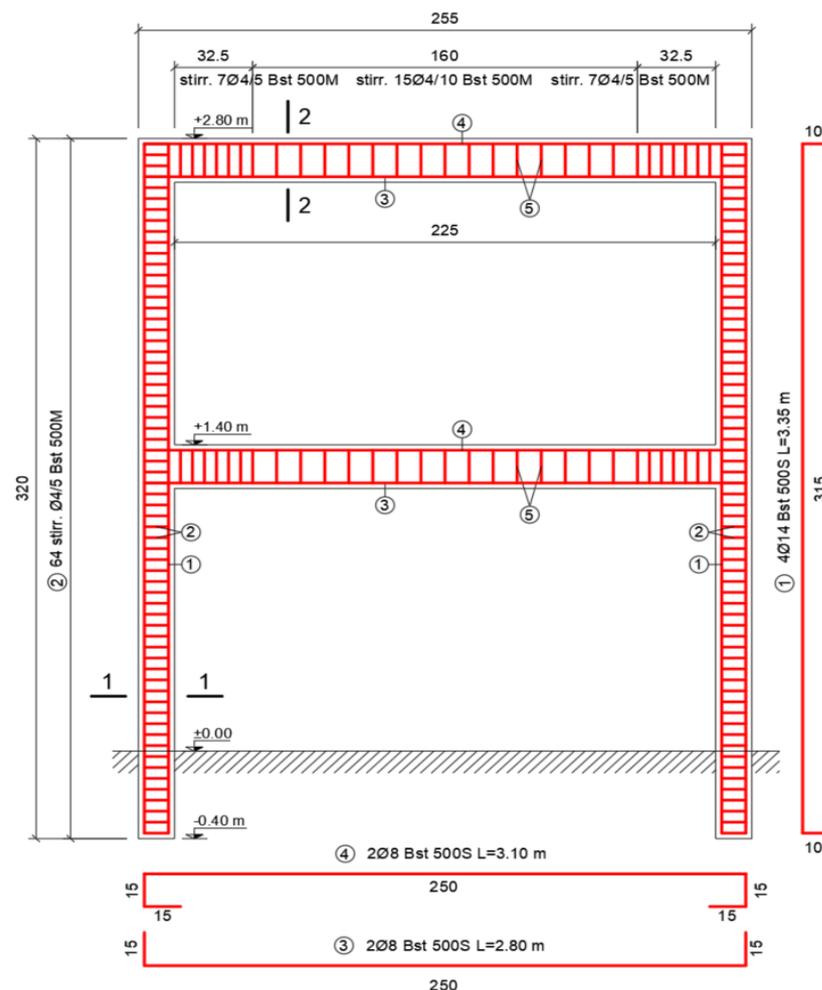

Figure 4. The representation of the reinforcement dispositions for columns and beams, on longitudinal direction, for the K_7; K_7_3_A; K_7_2_A; K_7_1_A and K_7_S_B_1 analytical MR RC frame models. The numbers in the circles are reinforcement marks, as one would find in a bill of quantities for steel reinforcement. (Note: The 1-1 and 2-2 cross sections of the RC beam and column can be studied in Figure 6).

Table 2. Principal aspects regarding the cross section reducing method of the RC beams through vertical drilling (mechanical) process in the marginal areas with potential plastic deformation for analytical MR RC frame models.

NSC	RC Drilled Element Type in the Potentially Plastic Zone	Hole Type Depends on the Geometric Shape (Form)	Variable (V)/Constant (C) Size Holes	Number of Holes	Number of Rows of Holes	Constant (C)/Variable (V) Distance between Holes	Constant (C)/Variable (V) Distance between Rows of Holes	Minimum (Min)/Maximum (Max) Distance between Holes and RC B-C Joint/RC Column	Rows of Vertical Holes Positioning (Zig-Zag, Parallel etc.)	GR
K_7	-	-	-	-	-	-	-	-	-	Figure 8(a1,a3)
K_7_3_A	beam	square holes	C	2 for LB 1 for TB	1 for LB 1 for TB	C	-	Min.	-	Figure 8(b1,b3)
K_7_2_A	beam	square holes	C	3 for LB 2 for TB	1 for LB 1 for TB	C	-	Min.	-	Figure 8(c1,c3)
K_7_1_A	beam	square holes	C	4 for LB 3 for TB	1 for LB 1 for TB	C	-	Min.	-	Figure 8(d1,d3)
K_7_S_B_1	beam and slab	square holes	C	4 for LB 3 for TB 6 for RC slab	1 for LB 1 for TB 2 for RC slab	C	- - C	Min.	- - parallel	Figure 8(e1,e3)

Note: Vertical holes were positioned between RC beams stirrups and RC slabs (steel) reinforcement bars, without structural integrity destruction of these structural elements. NSC—**N**umerical **S**imulation **C**ode; RC—**R**einforced **C**oncrete; LB—**L**ongitudinal **B**eams; TB—**T**ransverse **B**eams; CS—**C**ross **S**ection; GR—**G**raphical **R**epresentation.
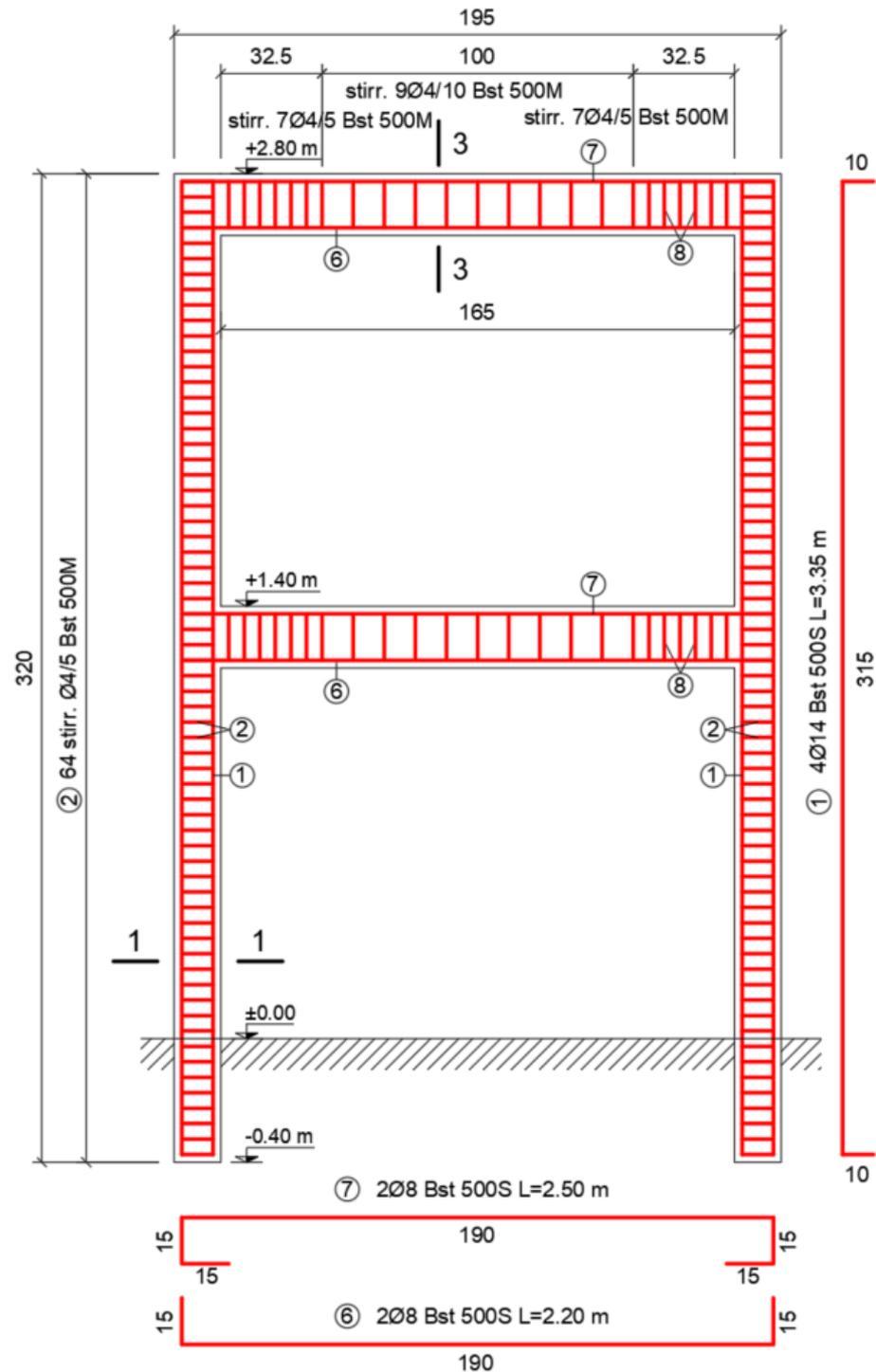
Figure 5. The representation of the reinforcement dispositions for columns and beams, on transversal direction, for the K_7; K_7_3_A; K_7_2_A; K_7_1_A and K_7_S_B_1 analytical MR RC frame models. The numbers in the circles are reinforcement marks, as one would find in a bill of quantities for steel reinforcement. (Note: The 1-1 and 3-3 cross sections of the RC beam and column can be studied in Figure 6).
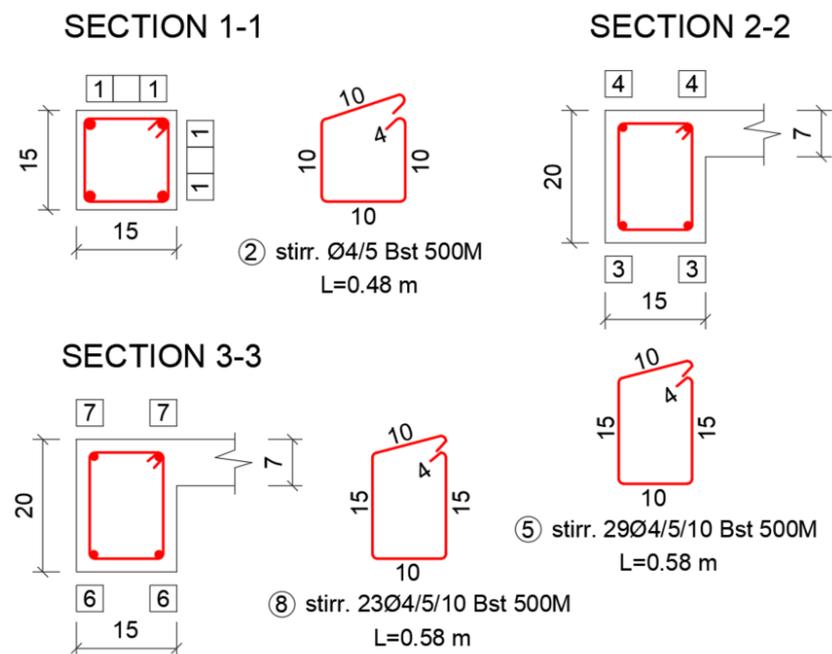
SECTION 1-1

SECTION 2-2

SECTION 3-3

Figure 6. The representation of 1-1, 2-2 and 3-3 cross sections of the RC beams and RC columns corresponding to the reinforcement "cage" depicted in Figures 4 and 5. The numbers in the circles are reinforcement marks, as one would find in a bill of quantities for steel reinforcement.
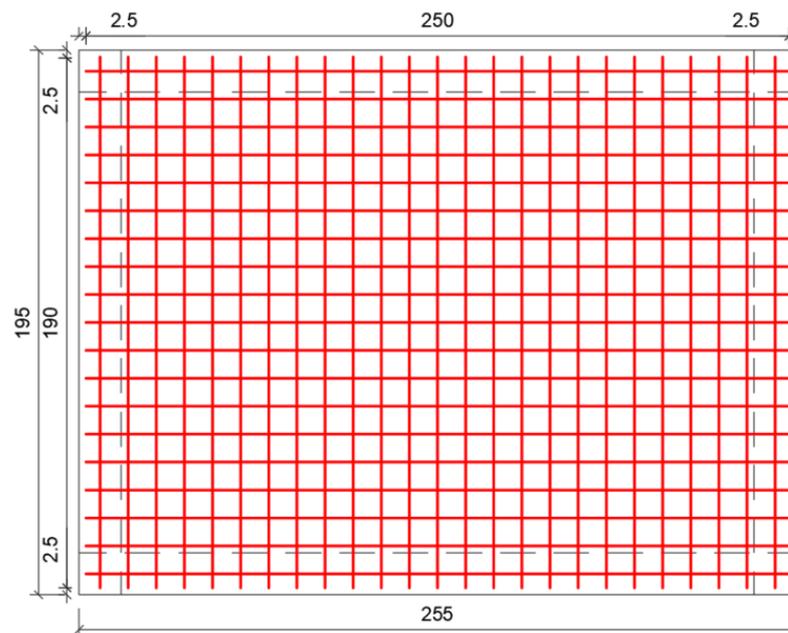

Figure 7. The representation of superior (P1 and P2) and inferior (P3 and P4) reinforcement mode of the slabs with welded wire mesh.

It should be noted that the current analytical study is part of a larger research project which includes the testing of a MR RC frame model on the shake table. Thus, the reduction to scale was performed according to the bearing capacity of the shake table as well as to the geometric in-plane restriction conditions.

For each of the studied analytical models, the "discretization rules" [52,53] (see Figure 3e), "stress-strain relations for concrete" [14,54–59] and "stress-strain laws for steel reinforcement" were observed and applied [14,60–63].

The way the current analytical study was approached, regarding the structural models for which the cross sections of the RC beams are reduced through mechanical drilling in zones where plastic deformation potential exists, stems from the idea of obtaining a mechanism exhibiting the "ductile seismic response" [49] of MR RC frame structures, i.e., with deformable beams in marginal zones and with columns with a linear elastic behaviour (see Figure 1b).

As such, this method may be viewed as a solution for the concentration and direction of plastic deformations in the marginal zones of the beams, such that the global plastic mechanism of MR RC frame structures will develop in its idealised form.

Therefore, for each type of analytical model, the parameters from Table 2 were considered, without taking into account the following specific detail elements:

- The influence of the geometric shape of the drilled holes regarding the local deformation mode of the structural element;
- The influence of the variability of the dimensions of the drilled holes regarding the local deformation mode of the structural element;
- the constant/variable distance between the drilled holes with the specified implicit value and the effect of such distances upon the local deformation mode of the structural element;
- The constant/variable distance between the rows of drilled holes with the specified implicit value and the effect of these distances upon the local deformation mode of the structural element;
- The distance from the node/column with the specified implicit value;
- The influence of the positioning of the rows of drilled holes in a zig-zag/parallel pattern, etc., upon the local deformation mode of the structural element.

The choice and the use of the set of parameters presented in Table 2 was carried out in order to simplify the analytical models generated with ATENA 3D.

Another desired simplification was the generation of the discretisation mesh, such that no issues would intervene regarding the "interaction between concrete and reinforcement bars" [52,53], etc.

The number of vertical drilled holes in the beams was established based on Lpl (where Lpl is the length of the plastic hinge in the RC beams, computed according to the P100-1 norm [1,64,65]) for superior limit for each direction, respectively for each type of beam: longitudinal, see Figure 4 and transversal, see Figure 5).

The same way of considering the vertical holes was used in the case of the RC slabs for the K_7_S_B_1 model.

The vertical holes were positioned between the stirrups of the beams/wire mesh of the slabs at a minimum distance from the beams/beam-column frame nodes (see Table 2). This minimum distance is dictated by the position of the first stirrup of the beams (Figures 4 and 5)/first wire mesh outside of the beam-column frame node (Figure 7).
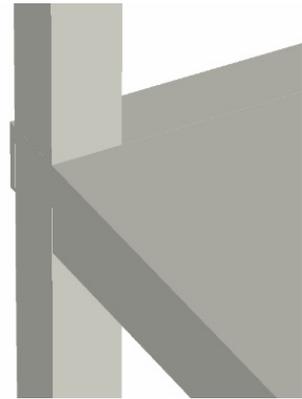
In Figure 8, the analytical models K_7, K_7_3_A, K_7_2_A, K_7_1_A and K_7_S_B_1 are presented in 3D format, including the zone pertaining to the beam-column frame node and the reinforcement configuration.
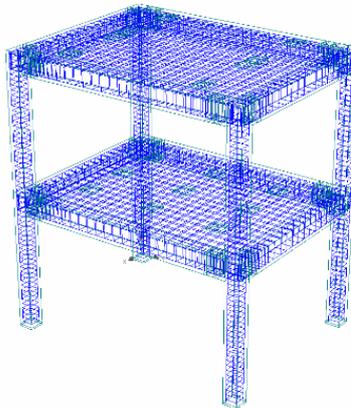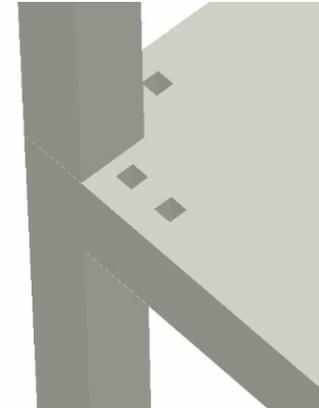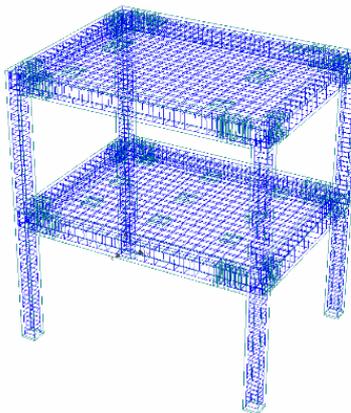
(**a1**)
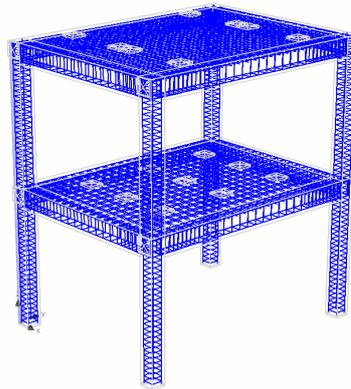
(**a2**)

(**a3**)

(**a**)

(**b1**)

(**b2**)

(**b3**)

(**b**)

(**c1**)

(**c2**)

(**c3**)

(c)

Figure 8. *Cont.*

(**d1**)　　　　　　　(**d2**)　　　　　　　(**d3**)

(**d**)

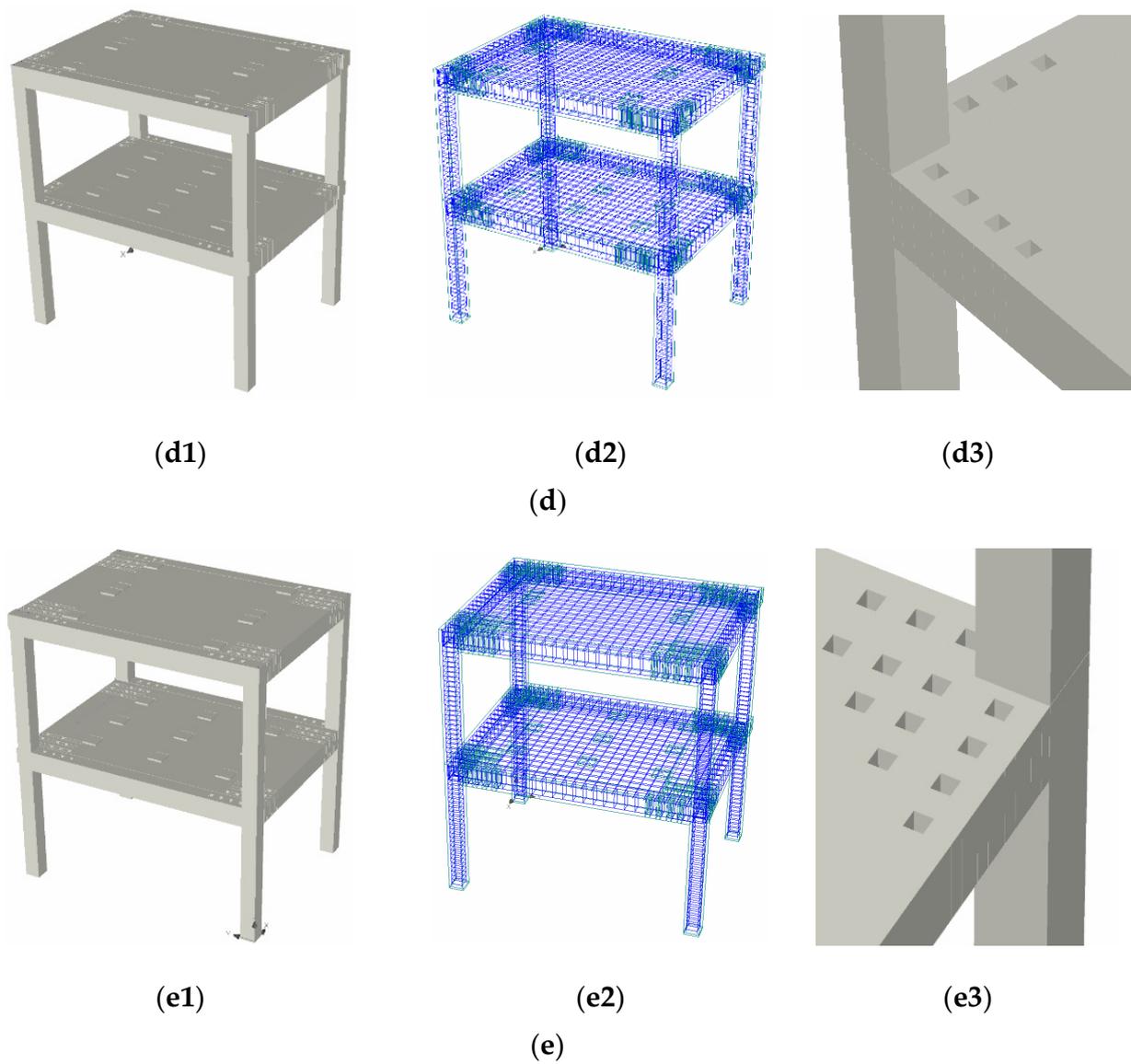(**e1**)　　　　　　　(**e2**)　　　　　　　(**e3**)

(**e**)
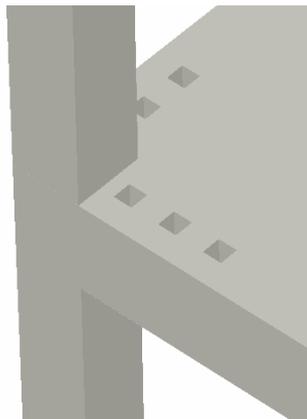
Figure 8. The graphic representation of the (**a**) K_7; (**b**) K_7_3_A; (**c**) K_7_2_A; (**d**) K_7_1_A; (**e**) K_7_S_B_1 analytical MR RC frame models: (**a1,b1,c1,d1,e1**) Global 3D representation of the structural system; (**a2,b2,c2,d2,e2**) "Steel reinforcement carcase in MR RC frame model" Reprinted from [13,15]; (**a3,b3,c3,d3,e3**) Local representation of the RC beam-column frame node at the slab over ground floor level (for all MR RC frame systems see Tables 1 and 2, Figures 3–7 and Figure 9).
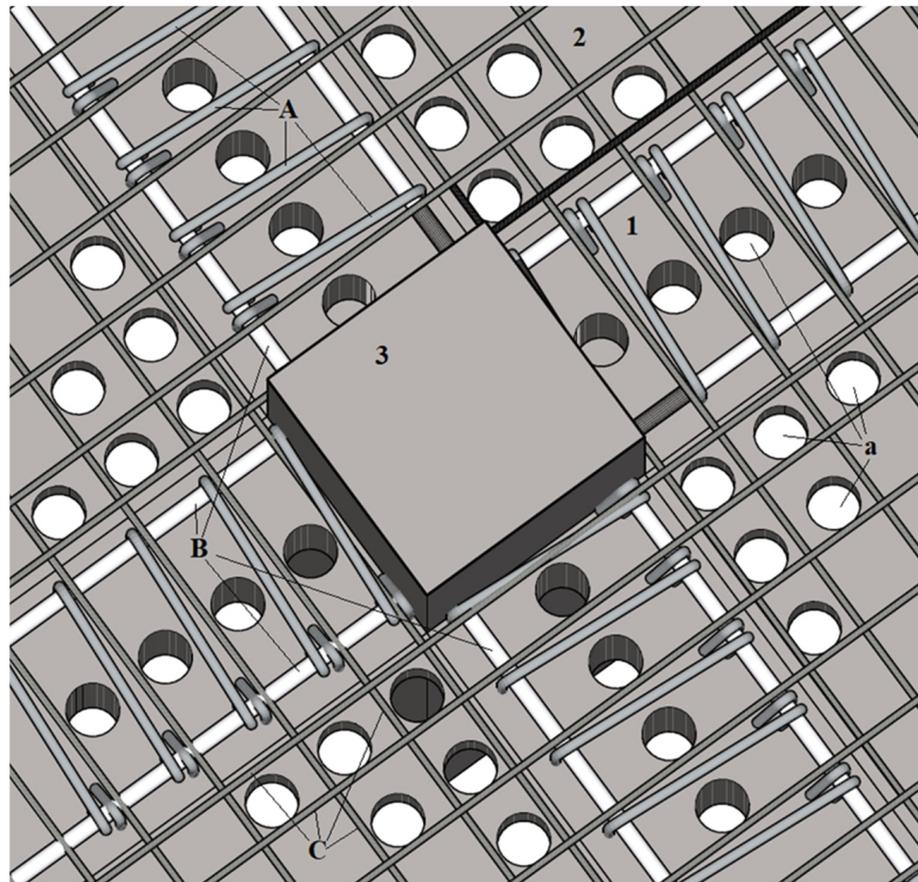
Figure 9. The disposition of vertical drilled holes in the end zones of the beams and in the corner zones of the RC slabs for K_7_S_B_1, K_7_3_A, K_7_2_A and K_7_1_A MR RC frame models, without any loss in structural integrity of the reinforcement bars, the beam-column frame node and the RC columns (1—RC beam; 2—RC slab; 3—RC columns; A—transversal reinforcement bars (stirrups) in RC beams; B—longitudinal reinforcement bars in RC beams; C—reinforcement wire meshes in the RC slabs; a—the geometric shape of the drilled holes) (Adapted from [66]). (Note: the geometric shape of the drilled holes considered for the analytical studies in the present paper is rectangular. The representation in Figure 9 has a purely informative character).

7. Analytical Results and Complementary Comments

7.1. Analytical Results

Following the non-linear static analyses for the cases specified in Tables 1 and 2 and Figure 8, regarding the MR RC frame models, the following data (results) were obtained (see Table 3 and Figures 10–14):

- Ultimate lateral force (Fu);
- Ultimate lateral displacement of the structural system (du);
- The lateral force corresponding to structural yielding of the equivalent SDOF structural system (F^*_y);
- The horizontal displacement at the top level of the structure corresponding to structural yielding of the equivalent SDOF structural system (d^*_y);
- The total specific deformations Eps zz;
- The main (maximum) failure deformations;
- The cracking panel for the final step of lateral loading.

Table 3. Analytical results in lateral forces, horizontal displacements and specific deformations for K_7, K_7_3_A, K_7_2_A, K_7_1_A and K_7_S_B_1 laterally loaded structural MR RC frame models with equivalent static forces.

NSC	F_u (kN)	d_u (m)	F^*_y (kN)	d^*_y (m)	SPO CB	TSE (CF)	TSE (TF)	GR TSE (CF/TF)	PFSM	GR PFSM
K_7	41.575	0.03288	40	0.0187	Figure 13a	0.002789	0.006118	Figure 14(a3,a4)	0.0413	Figure 14(a1,a2)
K_7_3_A	41.575	0.03109	40	0.0182	Figure 13c	0.002599	0.005614	Figure 14(b5,b6)	0.02547	Figure 14(b1–b4)
K_7_2_A	39.49625	0.0262	38.1	0.0167	Figure 13d	0.002072	0.003713	Figure 14(c5,c6)	0.01824	Figure 14(c1–c4)
K_7_1_A	39.49625	0.02665	38.1	0.0167	Figure 13e	0.002187	0.004011	Figure 14(d5,d6)	0.01959	Figure 14(d1–d4)
K_7_S_B_1	41.575	0.03179	40.4	0.0188	Figure 13b	0.002693	0.00576	Figure 14(e5,e6)	0.02913	Figure 14(e1–e4)

Note: NSC—**N**umerical **S**imulation **C**ode; F_u—ultimate lateral force corresponding to global system collapse; d_u—ultimate lateral displacement of the structural system; F^*_y—lateral force corresponding to structural yielding of the equivalent SDOF structural system; d^*_y –horizontal peak displacement corresponding to structural yielding of the equivalent SDOF structural system; SPO CB—**S**tatic **P**ush-**O**ver Curve **B**ilinearised; TSE—**T**otal **S**train **E**ps zz; CF—**C**ompressive **F**ailure; TF—**T**ensile **F**ailure; GR—**G**raphical **R**epresentation; PFSM—**P**rincipal **F**racture **S**train **M**ax. Specific deformations values in this table correspond to the final horizontal loading step. SPO curves for all MR RC frame models specified in the current table are graphically represented in Figure 10. **L**ateral **F**orces (LF)—PFSM curves for all MR RC frame models specified in the current table are graphically represented in Figure 11. LF—TSE curves for all MR RC frame models specified in the current table are graphically represented in Figure 12.
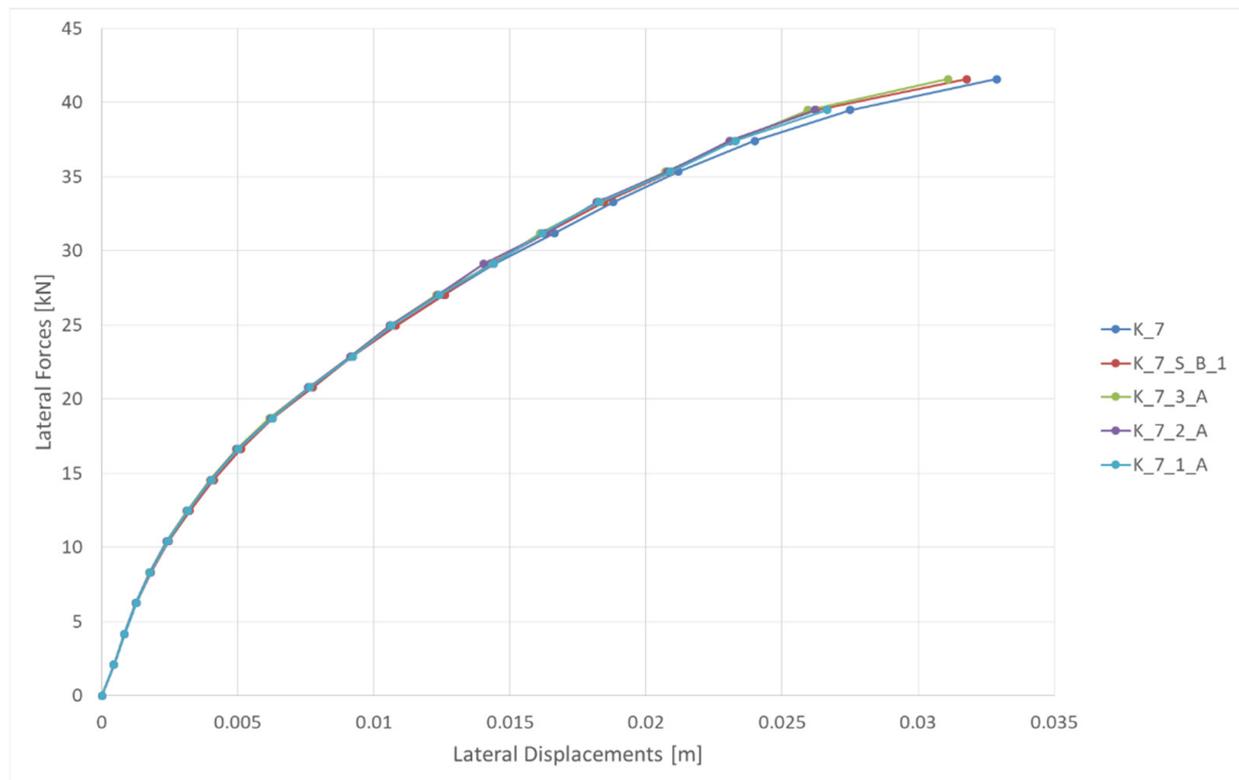

Figure 10. **S**tatic **P**ush-**O**ver (SPO) curves for K_7, K_7_S_B_1, K_7_3_A, K_7_2_A and K_7_1_A **M**oment **R**esisting (MR) **R**einforced **C**oncrete (RC) frame models.
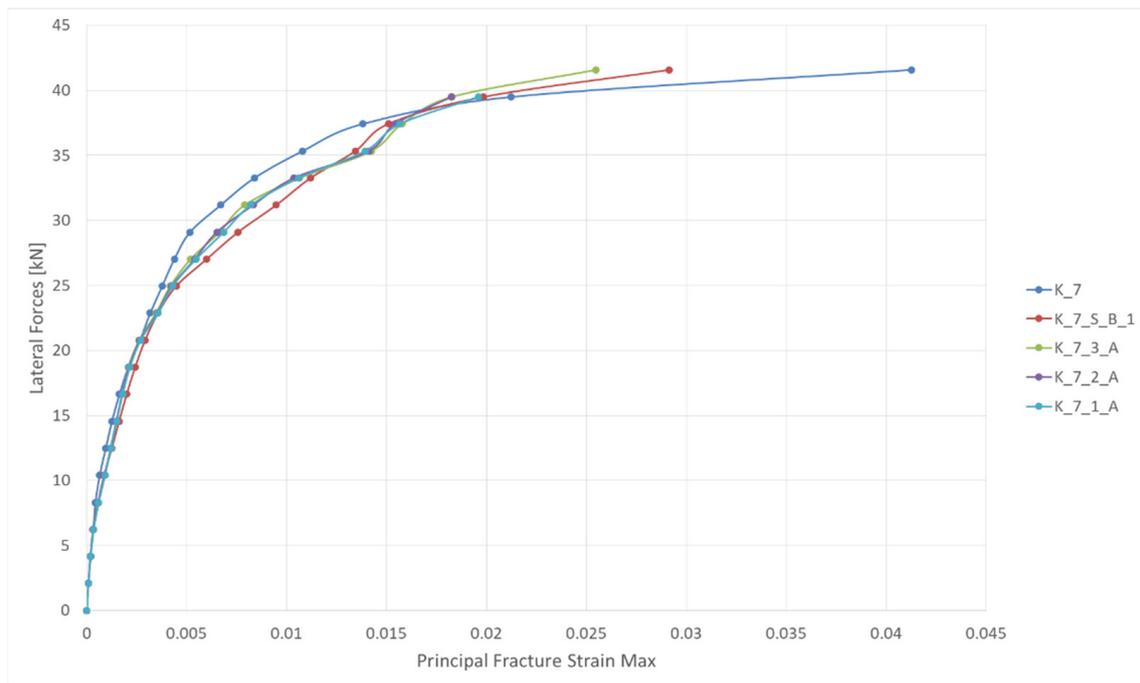
Figure 11. **L**ateral **F**orces (LF)—**P**rincipal **F**racture **S**trains **M**ax (PFSM) curves for K_7, K_7_S_B_1, K_7_3_A, K_7_2_A and K_7_1_A **M**oment **R**esisting (MR) **R**einforced **C**oncrete (RC) frame models.
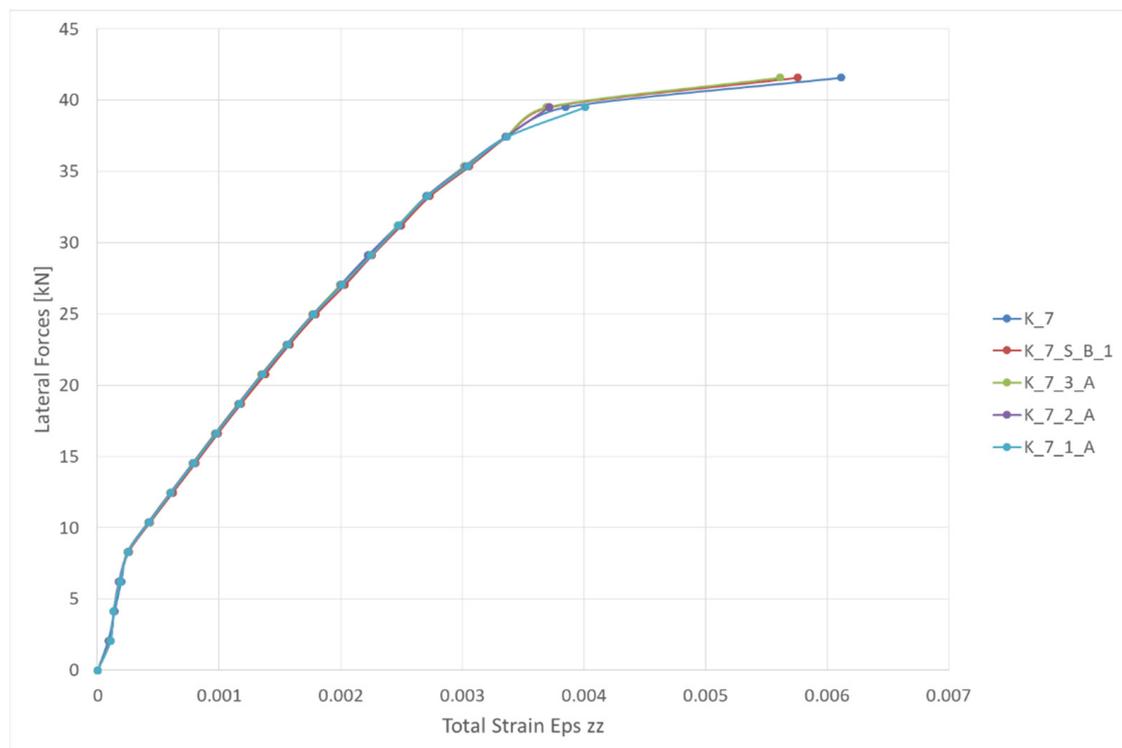
Figure 12. **L**ateral **F**orces (LF)—**T**otal **S**trains **E**ps zz (TSE) curves for K_7, K_7_S_B_1, K_7_3_A, K_7_2_A and K_7_1_A **M**oment **R**esisting (MR) **R**einforced **C**oncrete (RC) frame models.

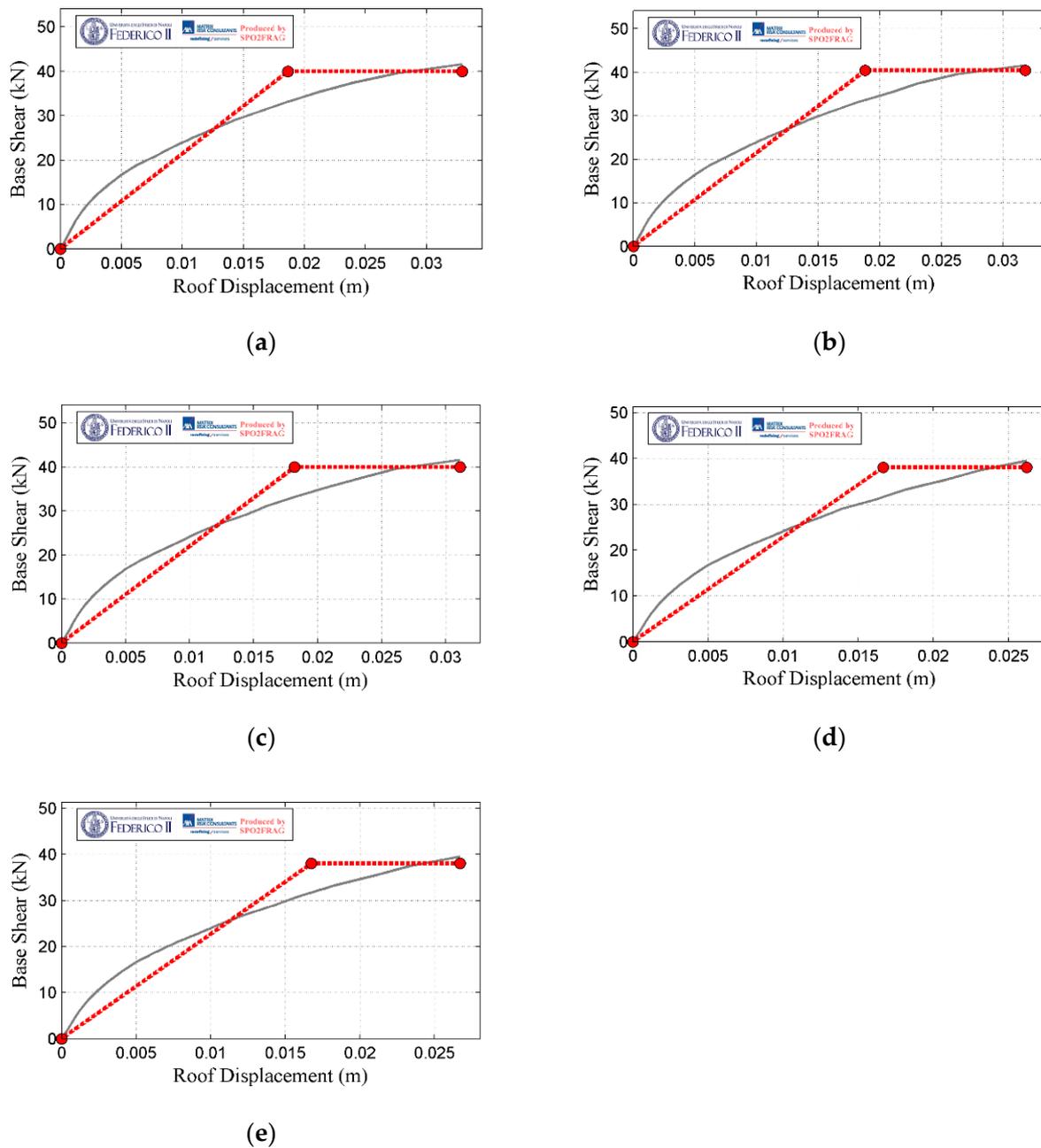**Figure 13.** Static Push-Over (SPO) curves (grey lines) and bilinearised curves (red lines) [67,68] (bilinearisation process according to elastic—perfectly plastic fit compatible with EC8 indications [2]) for: (**a**) K_7 [15]; (**b**) K_7_S_B_1; (**c**) K_7_3_A; (**d**) K_7_2_A; (**e**) K_7_1_A MR RC frame models. The implicit values of the SPO curves for the final step of lateral loading [69,70] can be studied in Table 3.

(**a1**)　　　　　　　　　　(**a2**)

(**a3**)　　　　　　　　　　(**a4**)

(**a5**)　　　　　　　　　　(**a6**)

(**a**)

Figure 14. *Cont.*

(**b1**)

(**b2**)

(**b3**)

(**b4**)

(**b5**)

(**b6**)

(**b**)

Figure 14. *Cont.*

(**c1**)

(**c2**)

(**c3**)

(**c4**)

(**c5**)

(**c6**)

(**c**)

Figure 14. *Cont.*

(**d1**)

(**d2**)

(**d3**)

(**d4**)

(**d5**)

(**d6**)

(**d**)

Figure 14. *Cont.*

(**e1**)

(**e2**)

(**e3**)

(**e4**)

(**e5**)

(**e6**)

(**e**)
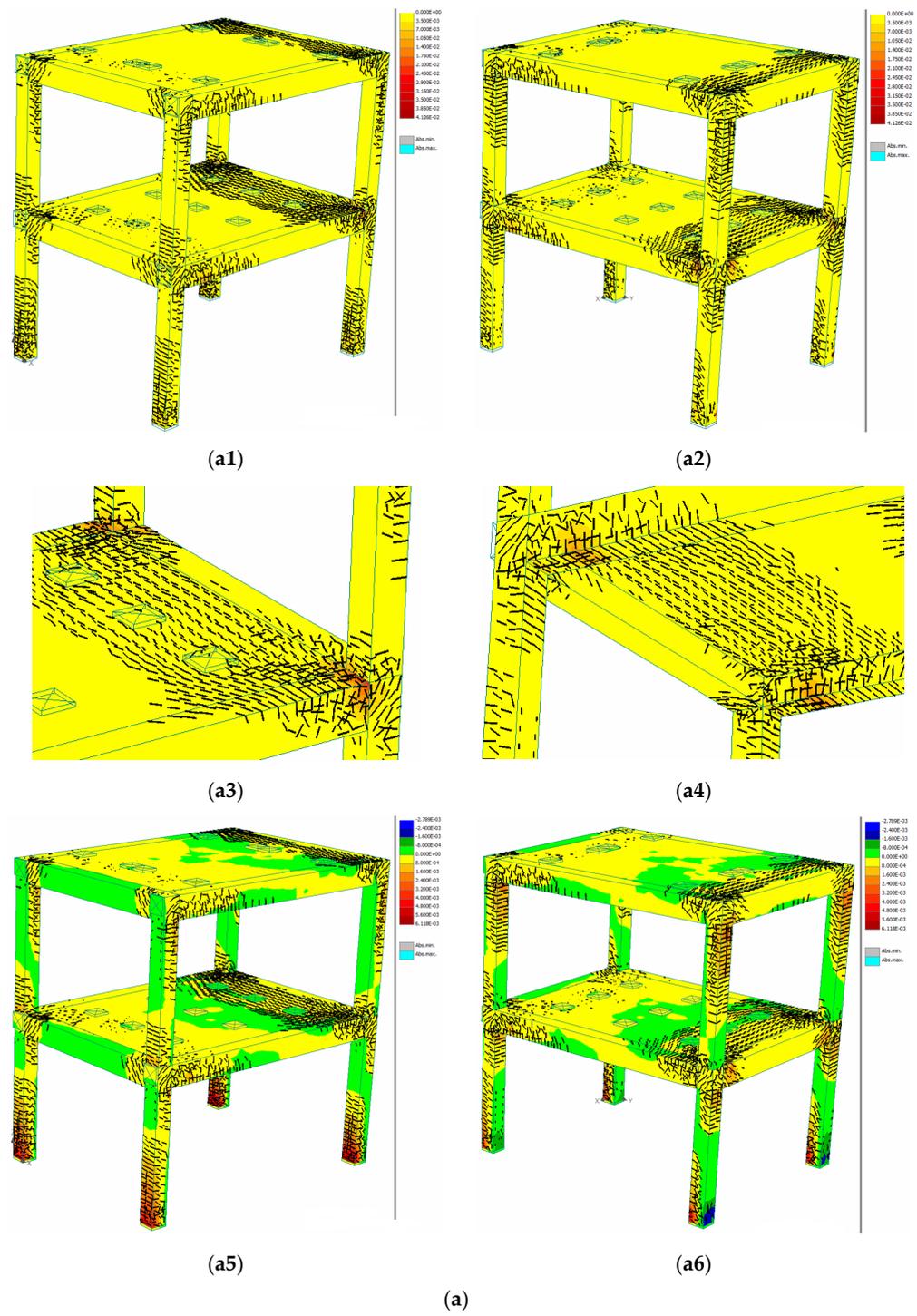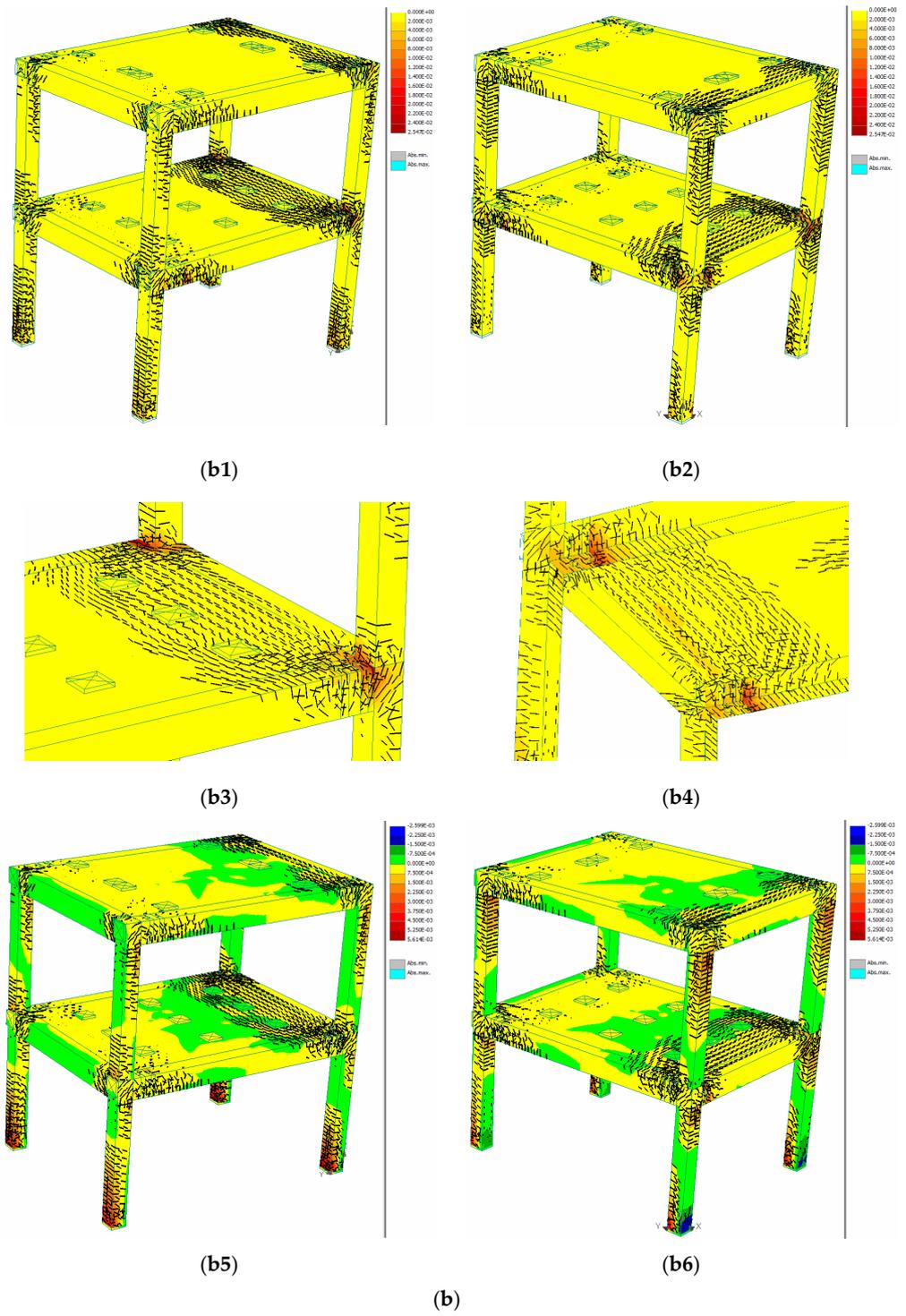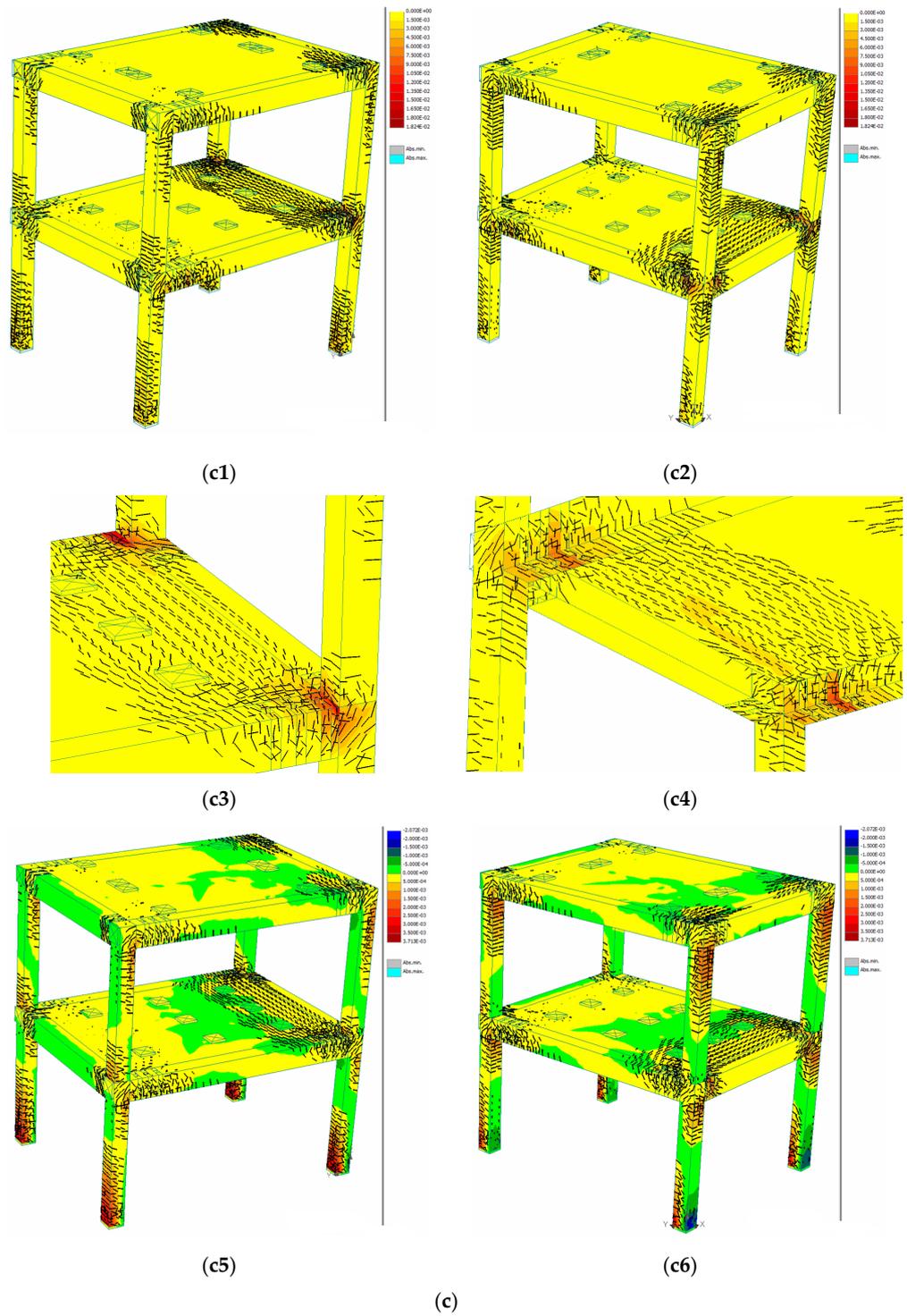
Figure 14. The graphical representation of the cracking mode of: (**a**) K_7 [15]; (**b**) K_7_3_A; (**c**) K_7_2_A; (**d**) K_7_1_A; (**e**) K_7_S_B_1 Moment Resisting (MR) Reinforced Concrete (RC) frame models for the ultimate lateral loading stage with: (**a1**,**a2**,**b1**,**b2**,**c1**,**c2**,**d1**,**d2**,**e1**,**e2**) Principal Fracture Strains Max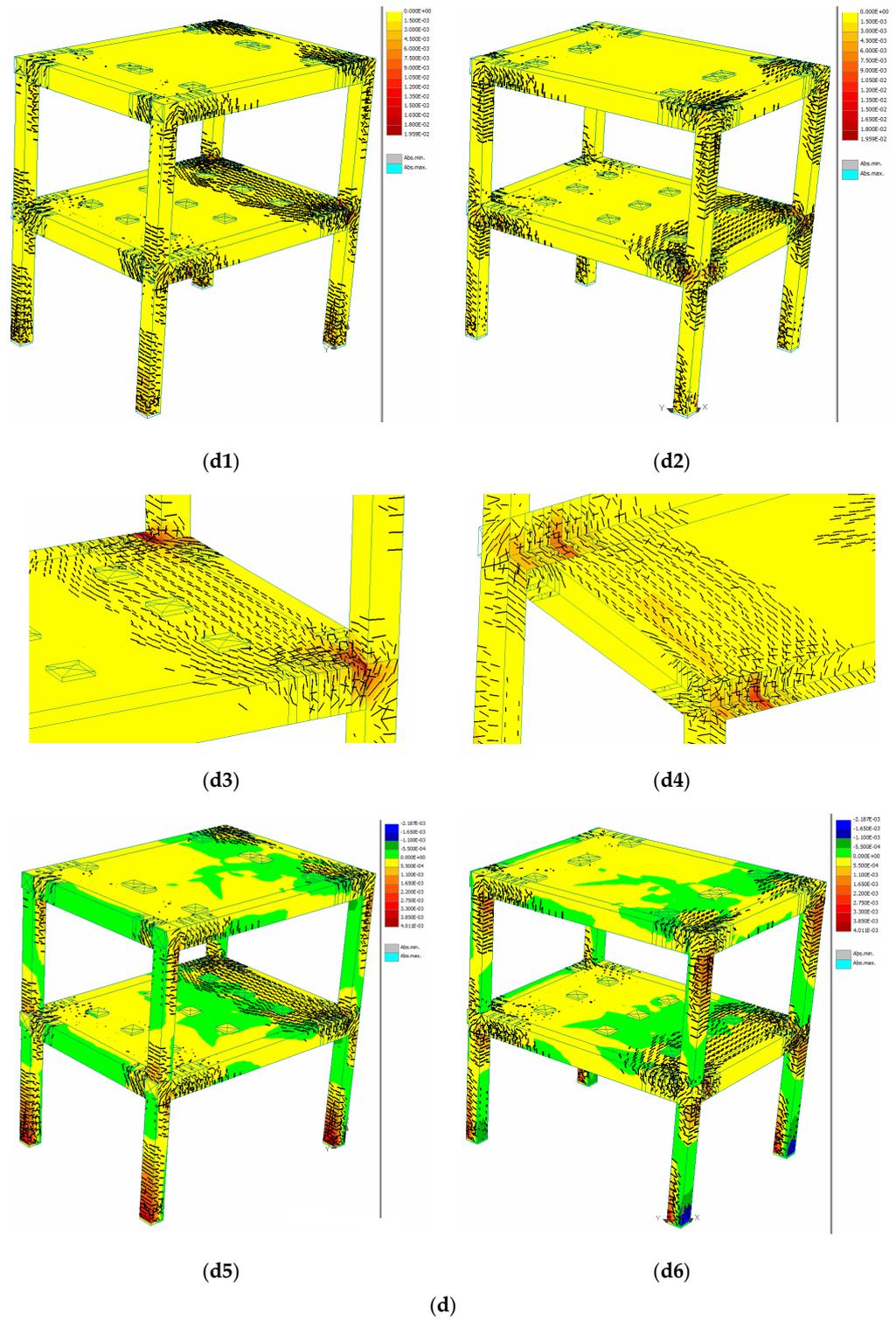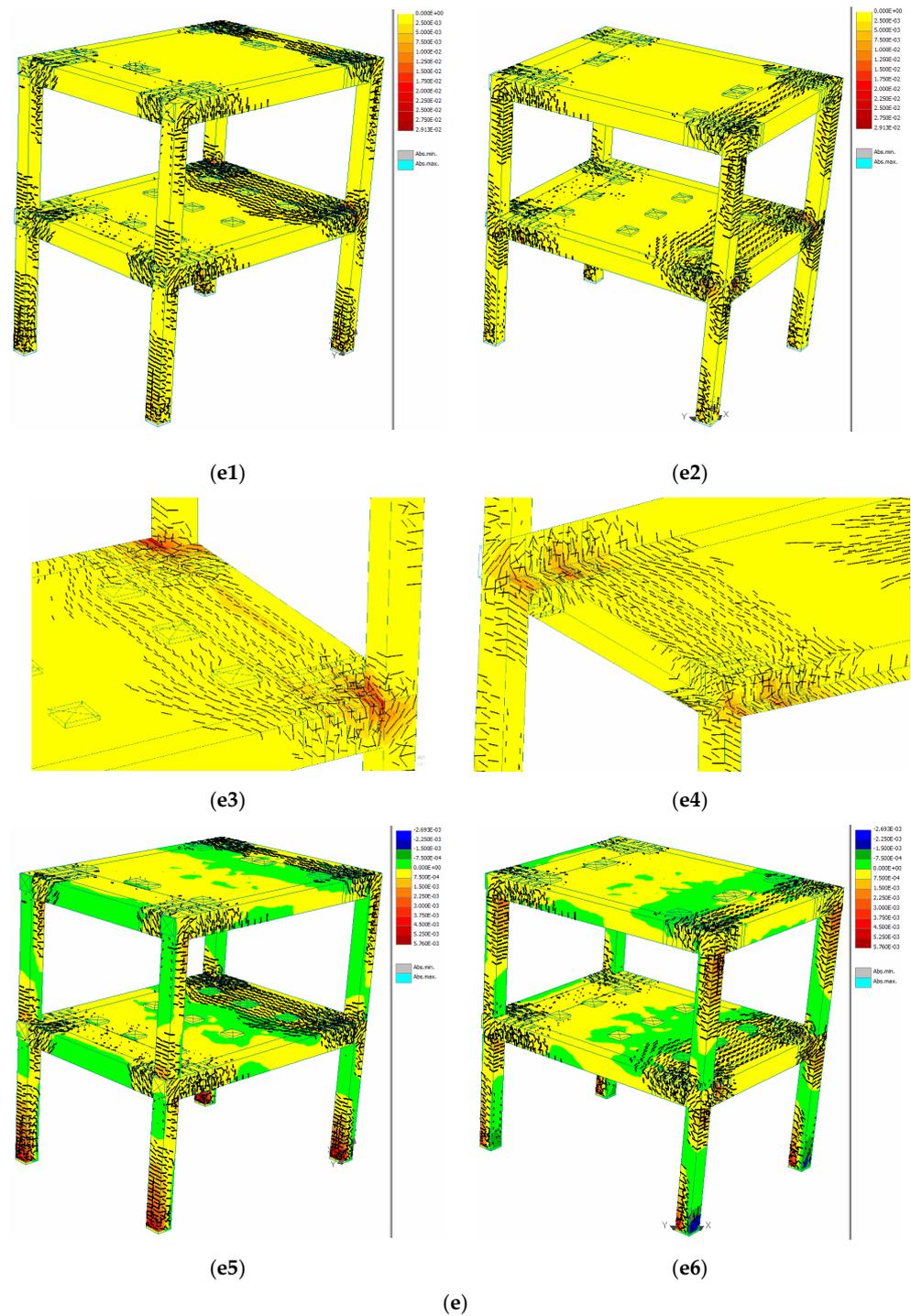 (PFSM) representations; (**a3**,**a4**,**b3**,**b4**,**c3**,**c4**,**d3**,**d4**,**e3**,**e4**) local Principal Fracture Strains Max (PFSM) representations; (**a5**,**a6**,**b5**,**b6**,**c5**,**c6**,**d5**,**d6**,**e5**,**e6**) Total Strains Eps zz (TSE) representations. (Note: In Table 3, the implicit PFSM and TSE values for the structural element zones with plastic deformation potential, which belong the analytical MR RC frame models (**a**–**e**), in the final step of lateral loading, are specified in a tabular format. In Figure 11, the PFSM values for each lateral loading step for the analytical RC frame models (**a**–**e**) are presented as curves. In Figure 12, the TSE values for each lateral loading step for the analytical MR RC frame models (**a**–**e**) are presented as curves).

The analytical results obtained following the non-linear static calculus are specified both in a tabular form (see Table 3) and as diagrams (see Figures 10–12) and were discussed in parallel with the graphical exposure of the cracking mode of each of the studied analytical model (see Figure 14). This was accompanied by the extraction of the effects and of the local seismic energy dissipation mechanisms for each of the structural element, in concert with the global mechanisms (for the entire structure).

The lateral forces F^*_y and the lateral displacements d^*_y corresponding to the structural yielding of the equivalent SDOF structural system were determined following a bilinearisation of the SPO capacity curves (see Figure 13) in accordance with the prescriptions found in Eurocode 8 [2]. The computer program SPO2FRAG was used in this process [67,68].

The general conclusions regarding the global and local seismic responses of the analysed RC frame models are presented in Table 4. The main failure mechanisms and other structural mechanisms which developed and were observed during the lateral loading of the structures are highlighted.

Thus, from the point of view of the seismic response at lateral forces and lateral displacements at the top of the structure, the K_7 and K_7_S_B_1 structural models registered the maximum values (see Table 3; Figure 10). Nevertheless, the structural yielding of the entire system varies for these two analytical models. Regarding the values of the specific failure deformations, the K_7 model is superior to K_7_S_B_1 model (see Figures 11 and 12). The other structural models which vary the number of vertical drilled holes in the end zones of the beams are positioned below the K_7 and K_7_S_B_1 analytical models, from the point of view of the values of the lateral forces, of lateral displacements (Figure 10), of specific failure deformations (Figure 11) and of total specific Eps zz deformations (Figure 12).

On the other hand, when graphically visualising the structural deformation process (mechanism), the model K_7 develops the least favourable mechanism of seismic energy dissipation, because it forms a common rigid block "slab-beams-frame node" (see Figure 14a). Furthermore, an excessive deformation of the beam-column frame node can be observed, together with large deformations in both marginal zones of the RC columns.

Compared with the seismic response of the K_7 model, the K_7_3_A, K_7_2_A and K_7_1_A models register a concrete cracking mechanism towards the weakened zones, i.e., towards the zones where the vertical drilled holes are present (Figure 14b–d). It can be thus stated that the concentration and direction process of the plastic hinges towards the drilled areas takes place (Figure 14(b3,b4,c3,c4,d3,d4)). For the analytical model which possesses the largest number of vertical drilled holes (K_7_1_A model), the optimum bending deformation shape of the RC beams is achieved (Figure 14d).

Additionally, the structural K_7_1_A and K_7_S_B_1 models exhibit the most favourable local deformation mechanisms for both concrete and steel, which favour the dissipation of the seismic energy.

As such, for these two structures, a mechanism of crack migration was observed. The cracks migrated from the zone of the longitudinal beam, which was weakened by drilling, towards the slab zone and towards the marginal zone (weakened also by drilled holes) of the transversal beam (on the short side of the structural system) (see Figure 14d,e).

In this way, the partial conservation mechanism for structural integrity of the beam-column frame node occurs. This is accompanied by an increase in the redundancy and in the ductility of the structural system, through the implication of a larger number of plastic zones (hinges).

Table 4. General aspects (conclusions) regarding the structural deformation response of the analytical MR RC frame models.

NSC	RC Beams Cracking Process		RC Columns Cracking Process		RC Slabs Cracking Process		RC Column-Beam Joint Cracking	Final Rupture—RC Structural Element/Elements	Zone/Zones of Final Rupture	RC Beam Cracking Length Limiting by RC Slab Cracking Area	Risk of the Common Rigid Block RC "Beam-Slab-Frame Node" Formation	Concrete Cracks Migration Process from the Longitudinal Beams to the Transverse Beams in the Adjacent Area of the Frame Node	GR
	Local—in Potential Plastic Zones	On Entire Length	Local—in Marginal Areas	On Entire Height	Local Area	Extended Area							
K_7	low	-	intense	low	low	medium to intense	intense	columns and nodes	marginal zones of the columns; entire volume of the nodes	yes	high with practical formation	low to insignificant	Figure 14a
K_7_3_A	medium	-	medium	low	low to medium	medium to intense	medium to intense	beams and nodes	marginal zones of the beams in reduced cross sections and immediately adjacent area of the beam-column joints	yes	medium with partial formation	low to medium	Figure 14b
K_7_2_A	medium to intense	-	medium	low	low to medium	medium to intense	medium to intense	beams and nodes	marginal zones of the beams in reduced cross sections and immediately adjacent area of the beam-column joints	yes	medium with partial formation	low to medium	Figure 14c
K_7_1_A	medium to intense	-	medium	low	medium	medium to intense	medium to intense	beams and nodes	marginal zones of the beams in reduced cross sections and immediately adjacent area of the beam-column joints	yes	medium with partial formation	low to medium	Figure 14d
K_7_S_B_1	medium to intense	-	medium	low	medium to intense	medium to intense	medium	beams, slabs and nodes	marginal zones of the beams in reduced cross sections; corner area for reduced cross section of the slabs; partial volume of the beam-column joints	partial with limited influence	medium with low process formation	medium to high	Figure 14e

Note: NSC—**N**umerical **S**imulation **C**ode; RC—**R**einforced **C**oncrete; GR—**G**raphical **R**epresentation. Specified conclusions in the current table were developed based on the recorded observations at each lateral loading step for each MR RC frame model. Specified figures in GR section (column) correspond to the seismic response of the MR RC frame systems (considered laterally loaded with equivalent static forces) in the ultimate horizontal loading step.

7.2. Complementary Comments

The numerical simulations corresponding to the analytical MR RC frame models prove the importance of the clear graphical specification of the deformation zone for each structural system. In the case where the graphical specification is not clear (regarding the precise trajectory of the cracks) and the obtained conclusions are based only on the capacity curves in Figure 10 or on other types of curves (Figures 11 and 12), a wrong interpretation of the global seismic response of the structure may occur. This is due to the complexity of deformation and structural cracking of reinforced concrete elements.

Moreover, the implicit value of the main failure deformations for any type of studied frame has a lower importance than the zone in which the maximum deformation itself occurs. This aspect can be particularly well observed in the K_7_1_A and K_7_S_B_1 models, for which the marginal zones of the beams which exhibit a plastic deformation potential became plastic zones following the lateral loading (see Figure 14d,e).

In addition to the above comments, the following aspects are specified:

- The number of drilled holes in the longitudinal and transversal RC beams influences the state of cracking/deformation of the zone with a plastic deformation potential, for each step of lateral loading. Consequently, for the K_7_1_A structural model in which the beams have a maximum number of drilled holes, the zones with plastic potential crack much faster (they exhibit important cracks from a lower loading step) and influence the deformation state of the RC slab. As the number of drilled holes in the beams decreases (as is the case for K_7_2_A and K_7_3_A models), the maximum main failure deformations affect the beam-column frame node and the RC column ends with a greater intensity (see Figure 14b,c).

- The number of vertical drilled holes considered in the corner zones of the RC slabs for the K_7_S_B_1 analytical frame model influences not only the structural cracking and deformation state of the respective zone (immediately adjacent to the drilled holes) with a plastic deformation potential, but also the cracking mode of the adjacent zones (i.e., the beam end zones) (Figure 14e). Additionally, the potentially plastic zones with vertically drilled holes in the corners of the slabs have become "migration zones" for the cracks/deformations from the longitudinal beams towards the transversal beams and towards the slab. This mechanism occurs in a shorter time (for a smaller number of lateral loading steps of the analytical model) and far more efficiently in comparison with the situation of the K_7 model. A part of the negative effects pertaining to the beam-column frame node and to the marginal zones of the RC columns is thus mitigated.

- The SPO curves presented in Figure 13 prove the incapacity for a complete visualisation of the global seismic response mode of the structures and can even lead to the obtainment of wrong conclusions. Thus, by analysing the bilinearised SPO curves from Figure 13, a conclusion that the unaffected model K_7 presents a global seismic response superior to the other analytical models may be reached.

The values of F^*_y lateral forces and of d^*_y lateral displacements corresponding to the structural yielding of the equivalent SDOF structural system for the K_7, K_7_S_B_1, K_7_3_A, K_7_2_A and K_7_1_A RC frame models, which can be found in Table 3, were determined following the bilinearisation of the SPO capacity curves in conformity with the prescriptions found in Eurocode 8 [2], with the SPO2FRAG computer program [67,68]. The representations of the bilinearised curves for each structural model may be consulted in Figure 13.

8. Conclusions

The general conclusions regarding the results of the analytical study pertaining to the applicability and validity of the practical method for improving the global and local seismic response by using the method of the reduction of the cross section of the RC beams through

mechanical drilling of vertical holes in the zones with a plastic deformation potential are summarised in Table 4.

The main local and/or global mechanisms of the analytical MR RC frame models studied in the present research paper, which were observed during the lateral step-by-step loading, are as follows:

- The guiding and concentration of the maximum failure deformations (PFSM) of concrete in the marginal ("weakened") areas of the beams with a reduced section (through the employment of vertically drilled holes) was achieved;
- The migration of cracks from the longitudinal beams to the transversal ones along the path of the corner zones of the drilled slabs was observed; as such, a partial "conservation" of the structural integrity (of strength and stiffness) of the beam-column frame node was accomplished;
- The failure of concrete and the reinforcement yielding in RC beam areas with a reduced section was noted;
- The interruption of the mechanism of development for the common rigid block "beams-slab-frame nodes" was achieved;
- The reduction of the cracking length influence of the slabs upon the cracking length of the reinforced concrete beams was observed;
- The reduction of the local destruction (failure) mechanism (effect) of the beam-column frame node was observed;
- The reduction of the mechanism (effect) of the plastic deformation concentration in the superior and inferior zones of the reinforced concrete columns was noted;
- The occurrence of complex seismic energy dissipation mechanisms through the registering of plastic deformations in beams, slabs and partially in frame nodes and end zones of the reinforced concrete columns was detected.

Despite these important observations, both the SPO curves and the bilinearised curves of the structural models associated with the tabular results with implicit values of the lateral forces and top displacements cannot offer a clear and realistic image regarding the structural seismic response.

Therefore, such a desirable and complete perspective should "capture" and describe the concrete failure mechanisms of the lateral system. This can only be achieved with the graphical knowledge of the accurate cracking and deformation mode at both the structural element level and at the lateral, interconnected elements level.

Hence, the proposed method of modifying the reinforced concrete beams through the reduction of the transversal (cross) section in zones with plastic deformation potential, such that the process of seismic energy dissipation in these specially designed zones will occur, is validated. Moreover, the negative effects induced by the superior bending stiffness of the slabs are limited.

It can be specified that the main objectives of the current analytical study were achieved:

- The integrity of the capacity and global design concept for the type of discussed structural system was achieved;
- The ductile mechanism "Strong Columns-Weak Beams" was partially achieved for the MR RC frame systems;
- The current design norms and regulations of seismic design for MR RC frame systems were respected;
- The base of this research included the real seismic response of reinforced concrete frame structures and the seismic response of the same type of structures discussed in other analytical studies.

References

1. *Cod de Proiectare Seismică", Partea I, Prevederi de Proiectare Pentru Clădiri, Indicativ P100-1, Ministerul Dezvoltării Regionale și Administrației Publice, Mai 2013*; UTCB: București, Romania, 2013. (In Romanian)
2. *Eurocod 8: Proiectarea Structurilor Pentru Rezistența la Cutremur, Partea 1: Reguli Generale, Acțiuni Seismice și Reguli Pentru Clădiri, Indicativ SR EN 1998-1*; ASRO: București, Romania, 2004. (In Romanian)
3. Paulay, T.; Priestley, M.J.N. *Seismic Design of Reinforced Concrete and Masonry Buildings*; John Wiley & Sons: New York, NY, USA, 1992.
4. Budescu, M.; Ciongradi, I. *Inginerie Seismică*; Politehnium: Iași, Romania, 2014. (In Romanian)
5. Postelnicu, T. *Proiectarea Structurilor de Beton Armat în Zone Seismice*; MarLink: București, Romania, 2012. (In Romanian)
6. Stratan, A. *Dinamica Structurilor și Inginerie Seismică*; Note de curs: Timișoara, Romania, 2014. (In Romanian)
7. Bai, J.; Ou, J. Plastic Limit-State Design of Frame Structures Based on the Strong-Column Weak-Beam Failure Mechanism. In Proceedings of the 15th World Conference on Earthquake Engineering, Lisboa, Portugal, 24–28 September 2012.
8. Ishiyama, Y. *Introduction to Earthquake Engineering and Seismic Codes in the World*; Hokkaido University: Hokkaido, Japan, 2011.
9. Akiyama, H. Collapse modes of structures under strong motions of earthquake. *Ann. Geophys.* **2002**, *45*, 791–798. [CrossRef]
10. Sococol, I.; Olteanu-Donțov, I.; Mihai, P.; Iftode, V.-I. Seismic response of $\frac{1}{2}$ scaled two storey reinforced concrete moment resisting frame system using nonlinear static analysis, Computational Civil Engineering (CCE 2021). *IOP Conf. Ser. Mater. Sci. Eng.* **2021**, *1141*, 012009. [CrossRef]
11. Sococol, I.; Mihai, P.; Toma, I.-O.; Venghiac, V.-M.; Olteanu-Dontov, I. Influence of Concrete Strength Class on the Plastic Hinges Location for a Reinforced Concrete Moment-Resisting Frame Structure with Consideration of the Horizontal Stiffening Effect of the Slab. *Bull. Polytech. Inst. Jassy Constr. Archit. Sect.* **2020**, *66*, 95–108.
12. Sococol, I.; Mihai, P.; Toma, I.-O.; Venghiac, V.-M.; Olteanu-Dontov, I. Static Non-linear Analysis of an RC Moment Resisting Frame by Considering Different Values for the Longitudinal Reinforcement Ratio in the Columns. *Bull. Polytech. Inst. Jassy Constr. Archit. Sect.* **2020**, *66*, 91–106.
13. Sococol, I.; Mihai, P.; Toma, I.-O.; Olteanu-Dontov, I.; Venghiac, V.-M. The Influence of the RC Beams Cross Section on the Dissipative Seismic Response of a Moment Resisting RC Frame System. *Bull. Polytech. Inst. Jassy Construction. Archit. Sect.* **2020**, *66*, 21–38.
14. Sococol, I.; Mihai, P.; Toma, I.-O.; Olteanu-Dontov, I.; Venghiac, V.-M. Stress-Strain Relation Laws for Concrete and Steel Reinforcement Used in Non-linear Static Analytical Studies of the Moment Resisting Reinforced Concrete (RC) Frame Models. *Bull. Polytech. Inst. Jassy Constr. Archit. Sect.* **2021**, *67*, 17–29. [CrossRef]
15. Sococol, I.; Petrescu, T.C.; Mihai, P.; Babor, D.T. Influence of the longitudinal steel ration in RC beams and steel reinforcement ration in RC slabs on the seismic energy dissipation mechanisms for a MR RC frame structure, Civil Engineering Conference. *IOP Conf. Ser. Mater. Sci. Eng.* 2022; Unpublished results-pending publication.
16. ATENA Software. Available online: http://www.cervenka.cz (accessed on 18 January 2021).
17. El-Attar, A.G.; White, R.N.; Gergely, P. *Shake Table Test of a 1/6 Scale Two-Story Lightly Reinforced Concrete Building*; Cornell University: New York, NY, USA, 1991.
18. Harris, H.G.; Sabnis, G.M. *Structural Modeling and Experimental Techniques, Second Edition*; CRC Press: Boca Raton, FL, USA, 1999.
19. Moncarz, P.D.; Krawinkler, H. *Theory and Application of Experimental Model Analysis in Earthquake Engineering*; Stanford University: San Jose, CA, USA, 1981.
20. Buildings Collapsed in IZMIR, Turkey after a Magnitude 6.9 Earthquake. Large Amount of Damage Reported throughout the City. 2020. Available online: https://turkey.liveuamap.com/en/2020/30-october-buildings-collapsed-in-izmir-turkey-after-a-magnitude (accessed on 26 April 2021).
21. The Ecuador Exchange: A Step Toward Earthquake-Resistant Cities. 2016. Available online: https://www.architectmagazine.com/practice/the-ecuador-exchange-a-step-toward-earthquake-resistant-cities_o2 (accessed on 26 April 2021).
22. Tzu Chi Begins Disaster Relief Assessment after Earthquake in Ecuador. 2016. Available online: https://tzuchi.us/blog/tzu-chi-begins-disaster-relief-assessment-after-earthquake-in-ecuador (accessed on 26 April 2021).
23. Kobe Earthquake of 1995. Available online: https://www.britannica.com/event/Kobe-earthquake-of-1995 (accessed on 26 April 2021).
24. Dalal, S.P.; Dalal, P. Strength, Deformation and Fragility assessment of Reinforced Concrete Moment Resisting frame designed by Force Based Design and the Performance Based Plastic Design method for Seismic loads. *Structures* **2021**, *29*, 1154–1164. [CrossRef]

25. Celik, O.C.; Ellingwood, B.R. Seismic fragilities for non-ductile reinforced concrete frames–Role of aleatoric and epistemic uncertainties. *Struct. Saf.* **2010**, *32*, 1–12. [CrossRef]

26. Arruda, M.R.T.; Castro, L.M.S. Non-linear dynamic analysis of reinforced concrete structures with hybrid mixed stress finite elements. *Adv. Eng. Softw.* **2021**, *153*, 102965. [CrossRef]

27. Belmouden, Y.; Lestuzzi, P. An equivalent frame model for seismic analysis of masonry and reinforced concrete buildings. *Constr. Build. Mater.* **2009**, *23*, 40–53. [CrossRef]

28. Brunesi, E.; Nascimbene, R.; Parisi, F.; Augenti, N. Progressive collapse fragility of reinforced concrete framed structures through incremental dynamic analysis. *Eng. Struct.* **2015**, *104*, 65–79. [CrossRef]

29. Brunesi, E.; Parisi, F. Progressive collapse fragility models of European reinforced concrete framed buildings based on pushdown analysis. *Eng. Struct.* **2017**, *152*, 579–596. [CrossRef]

30. Hu, B.; Lv, H.-L.; Kundu, T. Experimental study on seismic behavior of reinforced concrete frame in primary and middle schools with different strengthening methods. *Constr. Build. Mater.* **2019**, *217*, 473–486. [CrossRef]

31. U.S. Department of Homeland Security. *Assessing Seismic Performance of Buildings with Configuration Irregularities*; FEMA P-2012; Federal Emergency Management Agency: Oakland, CA, USA, 2018.

32. Sococol, I.; Toma, I.-O.; Mihai, P.; Țăranu, N.; Budescu, M. An Alternative Approach to Improve the Capacity Design Concept for Moment Resisting Reinforced Concrete (RC) Frame Systems. In Proceedings of the 1st Croatian Conference on Earthquake Engineering, Zagreb, Croatia, 22–24 March 2021; University of Zagreb Faculty of Civil Engineering: Zagreb, Croatia, 2021. [CrossRef]

33. Yan, L.; Gong, J. Development of displacement profiles for direct displacement based seismic design of regular reinforced concrete frame structures. *Eng. Struct.* **2019**, *190*, 223–237. [CrossRef]

34. Wang, H.; Su, Y.; Zeng, Q. Design Methods of Reinforce-concrete Frame Structure to Resist Progressive Collapse in Civil Engineering. In Proceedings of the 2011 International Conference on Risk and Engineering Management (REM), Toronto, ON, Canada, 28–30 October 2011; p. 7.

35. The Japan Building Disaster Prevention Association. *Standard for Seismic Evaluation of Existing Reinforced Concrete Buildings, Guidelines for Seismic Retrofit of Existing Reinforced Concrete Buildings, Technical Manual for Seismic Evaluation and Seismic Retrofit of Existing Reinforced Concrete Buildings*, 1st ed.; BRI, English Version; JICA: Osaka, Japan, 2001.

36. Lists of 21st-Century Earthquakes. 2021. Available online: https://en.wikipedia.org/wiki/Lists_of_21st-century_earthquakes (accessed on 26 April 2021).

37. Japan, Researchers Test 10-Storey Concrete Building for Resilience Against 'New Kobe Earthquake'. 2015. Available online: https://www.ibtimes.co.uk/japan-researchers-test-10-storey-concrete-building-resilience-against-new-kobe-earthquake-1532970 (accessed on 26 April 2021).

38. Wang, D.; Li, H.-N.; Li, G. Experimental tests on reinforced concrete columns under multi-dimensional dynamic loadings. *Constr. Build. Mater.* **2013**, *47*, 1167–1181. [CrossRef]

39. Taheri, A.; Tasnimi, A.A.; Moghadam, A.S. Experimental investigation on the seismic behavior and damage states of reinforced high strength concrete columns. *Structures* **2020**, *27*, 163–173. [CrossRef]

40. Li, Y.; Yin, S.; Dai, J.; Liu, M. Numerical investigation on the influences of different factors on the seismic performance of TRC-strengthened RC columns. *J. Build. Eng.* **2020**, *30*, 101245. [CrossRef]

41. Zembaty, Z.; Kowalski, M.; Pospisil, S. Dynamic identification of a reinforced concrete frame in progressive states of damage. *Eng. Struct.* **2006**, *28*, 668–681. [CrossRef]

42. Kamath, P.; Sharma, U.K.; Kumar, V.; Bhargava, P.; Usmani, A.; Singh, B.; Singh, Y.; Torero, J.; Gillie, M.; Pankaj, P. Full-scale fire test on an earthquake-damaged reinforced concrete frame. *Fire Saf. J.* **2015**, *73*, 1–19. [CrossRef]

43. Rizwan, M.; Ahmad, N.; Khan, A.N. Seismic performance assessment of reinforced concrete moment resisting frame with low strength concrete. *Structures* **2021**, *30*, 1140–1160. [CrossRef]

44. Pohoryles, D.A.; Melo, J.; Rossetto, T.; Varum, H.; D'Ayala, D. Effect of slab and transverse beam on the FRP retrofit effectiveness for existing reinforced concrete structures under seismic loading. *Eng. Struct.* **2021**, *234*, 111991. [CrossRef]

45. Li, S.; Zuo, Z.; Zhai, C.; Xu, S.; Xie, L. Shaking table test on the collapse process of a three-story reinforced concrete frame structure. *Eng. Struct.* **2016**, *118*, 156–166. [CrossRef]

46. Hou, S.; Zhang, H.; Han, X.; Ou, J. Damage monitoring of the RC frame shaking table test and comparison with FEM results. *Procedia Eng.* **2017**, *210*, 393–400. [CrossRef]

47. Zhang, H.; Li, H.-N.; Li, C.; Cao, G.-W. Experimental and numerical investigations on seismic responses of reinforced concrete structures considering strain rate effect. *Constr. Build. Mater.* **2018**, *173*, 672–686. [CrossRef]

48. Liu, J.; Zhang, J.; Li, X.; Cao, W. Cyclic behavior of damage-controllable steel fiber reinforced high-strength concrete reduced-scale frame structures. *Eng. Struct.* **2021**, *232*, 111810. [CrossRef]

49. Sococol, I.; Mihai, P.; Olteanu-Dontov, I. Ductility–Concept for Improving the Seismic Response for Structural Reinforced Concrete Frame Systems, Bulletin of the Polytechnic Institute of Jassy. *Constr. Archit. Sect.* **2019**, *65*, 17–30.

50. Cervenka, V.; Jendele, L.; Cervenka, J. *ATENA Program Documentation. Part 1. Theory*; Cervenka Consulting Ltd.: Prague, Czech Republic, 2012.

51.　Sococol, I.; Mihai, P.; Iftode, V.I.; Olteanu-Dontov, I. Study Regarding the Stiffness Influence of Slab to Beams for a Plan Structural Reinforced Concrete Frame System in Seismic Zones. In Proceedings of the Computational Civil Engineering Conference, CCE, Iasi, Romania, 30–31 May 2019; Materials Science and Engineering. IOP Publishing: Bristowl, UK, 2019; Volume 586. [CrossRef]

52.　Bitencourt, L.A.G., Jr.; Manzoli, O.L.; Trindade, Y.T.; Rodrigues, E.A.; Dias-da-Costa, D. Modeling reinforced concrete structures using coupling finite elements for discrete representation of reinforcements. *Finite Elem. Anal. Des.* **2018**, *149*, 32–44. [CrossRef]

53.　Sousa, J.B.M., Jr.; Muniz, C.F.D.G. Analytical integration of cross section properties for numerical analysis of reinforced concrete, steel and composite frames. *Eng. Struct.* **2007**, *29*, 618–625. [CrossRef]

54.　Kupfer, H.; Hilsdorf, H.K.; Rusch, H. Behavior of Concrete under Biaxial Stress. *J. ACI* **1969**, *66*, 656–666.

55.　Shiming, S.; Yupu, S. Dynamic biaxial tensile-compressive strength and failure criterion of plain concrete. *Constr. Build. Mater.* **2013**, *40*, 322–329. [CrossRef]

56.　Ivashenko, Y.; Ferder, A. Experimental studies on the impacts of strain and loading modes on the formation of concrete "stress-strain" relations. *Constr. Build. Mater.* **2019**, *209*, 234–239. [CrossRef]

57.　Bi, J.; Huo, L.; Zhao, Y.; Qiao, H. Modified the smeared crack constitutive model of fiber reinforced concrete under uniaxial loading. *Constr. Build. Mater.* **2020**, *250*, 118916. [CrossRef]

58.　Wei, H.; Wu, T.; Liu, X.; Zhang, R. Investigation of stress-strain relationship for confined lightweight aggregate concrete. *Constr. Build. Mater.* **2020**, *256*, 119432. [CrossRef]

59.　Dong, S.; Wang, Y.; Ashour, A.; Han, B.; Ou, J. Uniaxial compressive fatigue behavior of ultra-high performance concrete reinforced with super-fine stainless wires. *Int. J. Fatigue* **2021**, *142*, 105959. [CrossRef]

60.　Xu, T.; Castel, A.; Gilbert, R.I.; Murray, A. Modeling the tensile steel reinforcement strain in RC-beams subjected to cycles of loading and unloading. *Eng. Struct.* **2016**, *126*, 92–105. [CrossRef]

61.　Wang, Z.-H.; Li, L.; Zhang, Y.-X.; Zheng, S.-S. Reinforcement model considering slip effect. *Eng. Struct.* **2019**, *198*, 109493. [CrossRef]

62.　Long, X.; Wang, C.-Y.; Zhao, P.-Z.; Kang, S.-B. Bond strength of steel reinforcement under different loading rates. *Constr. Build. Mater.* **2020**, *238*, 117749. [CrossRef]

63.　Sabău, M. Simulated data on bond of steel reinforcement in self-compacting concrete. *Data Brief* **2020**, *30*, 105594. [CrossRef]

64.　*CEB-FIP Model Code 1990*; First Draft; Committee Euro-International du Beton: Lausanne, Switzerland, 1990; Available online: http://www.tocasa.es/zona2/CEB_FIP_model_code_1990_ing.pdf (accessed on 26 April 2021).

65.　*Eurocod 2: Proiectarea Structurilor de Beton, Partea 1-1: Reguli Generale și Reguli Pentru Clădiri, INDICATIV SR EN 1992-1-1*; ASRO: București, Romania, 2006. (In Romanian)

66.　Tehnică, U.; Asachi, G.; Iași, D. Grindă și placă pentru disipare de energie seismică. Patent Application A/00045, 12 February 2021. (In Romanian).

67.　Baltzopoulos, G.; Baraschino, R.; Iervolino, I.; Vamvatsikos, D. SPO2FRAG: Software for seismic fragility assessment based on static pushover. *Bull. Earthq. Eng.* **2017**, *15*, 4399–4425. [CrossRef]

68.　Baltzopoulos, G.; Baraschino, R.; Iervolino, I.; Vamvatsikos, D. *SPO2FRAG [Computer Software]. AXA-DiSt*; Universita Degli Studi di Napoli Federico II: Naples, Italy, 2017.

69.　Li, H.; Yi, T.; Gu, M.; Huo, L. Evaluation of earthquake-induced structural damages by wavelet transform. *Prog. Nat. Sci.* **2009**, *19*, 461–470. [CrossRef]

70.　Lin, S.-W.; Yi, T.-H.; Li, H.-N.; Ren, L. Damage Detection in the Cable Structures of a Bridge Using the Virtual Distortion Method. *J. Bridge Eng.* **2017**, *22*, 04017039. [CrossRef]